

1 Updated Growth Models for Bigeye Tuna (*Thunnus obesus*) in the Atlantic Ocean

2 By

3 Lynn Waterhouse<sup>1,2</sup>, Lisa Ailloud<sup>3,4</sup>, Riley Austin<sup>5</sup>, Walter J. Golet<sup>5</sup>, Ashley Pacicco<sup>6</sup>, Allen H.  
4 Andrews<sup>7</sup>, Khady Diouf<sup>8</sup>, Yacine Ndiour<sup>8</sup>, Kyne Krusic-Golub<sup>9</sup>, Guelson da Silva<sup>10</sup>, and John M.  
5 Hoenig<sup>11</sup>

6  
7 1. Past affiliation: John G. Shedd Aquarium, 1200 South Lake Shore Drive, Chicago, IL 60605,  
8 USA. [waterhlz@gmail.com](mailto:waterhlz@gmail.com)

9 2. Present address: Minnesota Cooperative Fish and Wildlife Research Unit, University of  
10 Minnesota, Department of Fisheries, Wildlife, and Conservation Biology, 1980 Folwell Avenue,  
11 St. Paul, MN 55108, USA. [lwater@umn.edu](mailto:lwater@umn.edu)

12 3. Past affiliation: ICCAT Secretariat, Calle Corazón de Maria 8, 28002 Madrid, Spain.

13 4. Present address: National Marine Fisheries Service, Southeast Fisheries Science Center, 75  
14 Virginia Beach Drive, Miami, FL 33149, USA. [lisa.ailloud@noaa.gov](mailto:lisa.ailloud@noaa.gov)

15 5. The University of Maine – Gulf of Maine Research Institute, School of Marine Sciences 350  
16 Commercial Street, Portland, ME 04101, USA. [Walter.golet@maine.edu](mailto:Walter.golet@maine.edu) [riley.austin@maine.edu](mailto:riley.austin@maine.edu)

17 6. Cooperative Institute for Marine and Atmospheric Studies, Rosenstiel School for Marine and  
18 Atmospheric Science, University of Miami, FL 33149, USA. [Ashley.pacicco@noaa.gov](mailto:Ashley.pacicco@noaa.gov)

19 7. University of Hawaii at Manoa, Department of Oceanography, 1000 Pope Road, Honolulu, HI  
20 96822, USA. [astrofish226@gmail.com](mailto:astrofish226@gmail.com)

21 8. Institute fondamentale Afrique noire Cheikh Anto Diop - Corniche Ouest - Université Cheikh  
22 Anta Diop, BP 206 Dakar-Fann, Dakar, Senegal. [khady1.diouf@ucad.edu.sn](mailto:khady1.diouf@ucad.edu.sn)  
23 [yasminandiour@gmail.com](mailto:yasminandiour@gmail.com)

24 9. Fish Ageing Services, 28 Swanston St, Queenscliff, 3225, VIC, Australia  
25 [kyne.krusicgolub@fishageingservices.com](mailto:kyne.krusicgolub@fishageingservices.com)

26 10. Departamento de Ciências Animais, Universidade Federal Rural do Semiárido, Mossoro,  
27 Brazil. [guelson@ufersa.edu.br](mailto:guelson@ufersa.edu.br)

28 11. Virginia Institute of Marine Science, College of William & Mary, P.O. Box 1346, Gloucester  
29 Point, VA 23062, USA. [hoenig@vims.edu](mailto:hoenig@vims.edu)

30

31

32

33 **Abstract**

34 The International Commission for the Conservation of Atlantic Tunas (ICCAT) concluded the  
35 Atlantic Ocean tropical Tuna Tagging Programme (AOTTP) in 2021. This project had the  
36 objectives of enhancing food security, stimulating economic growth, and improving management  
37 through research on tropical tuna resources in the Atlantic Ocean, including bigeye tuna  
38 (*Thunnus obesus*). Here, we combine tagging data and otolith data from the AOTTP program,  
39 Panama City Lab and the Pelagic Fisheries Lab at the University of Maine with historical  
40 tagging data and otolith data from ICCAT and other sources to fit integrated growth models with  
41 the goal of providing the most complete growth curve (in terms of data inclusion and validation  
42 of age-at-length) for bigeye tuna in the Atlantic Ocean. Both Richards and von Bertalanffy  
43 growth models were fitted. A variety of models were fitted to subsets of the data to investigate  
44 the consistency of growth information. In all cases for the integrated model, the Richards and  
45 von Bertalanffy models were very similar with the von Bertalanffy model being preferred for  
46 parsimony. The preferred model, based on fit to old fish, was the von Bertalanffy curve based on  
47 length-age pair data from multiple sources. The addition of tagging data to create an integrated  
48 model showed patterns of lack of fit to both the tagging and otolith data suggesting conflict  
49 between the tagging and otolith data. The preferred model (length-age pair data only) gave the  
50 estimates: asymptotic length  $L_{\infty}$  (fork length) equals 161.21 cm (95% bootstrap CI 154.39,  
51 166.84), growth parameter  $K$  equals  $0.392 \text{ yr}^{-1}$  (95% bootstrap CI 0.355, 0.441), and the time-  
52 axis intercept  $t_0$  equals  $-0.239 \text{ yr}$  (95% bootstrap CI  $-0.306, -0.175$ ). For the best fitting  
53 integrated model, the asymptotic length  $L_{\infty}$ (fork length, in cm) was estimated to be 185.78 (SD  
54 6.298), the growth parameter  $K$  was  $0.252 \text{ yr}^{-1}$  (SD 0.014), and the time-axis intercept  $t_0$  was -  
55 0.524 yr (SE 0.025). The value for asymptotic length  $L_{\infty}$  from the integrated model was larger  
56 than the lengths of all the old fish in the sample whereas the value for the curve based on otoliths  
57 passes through the cloud of points for old fish.

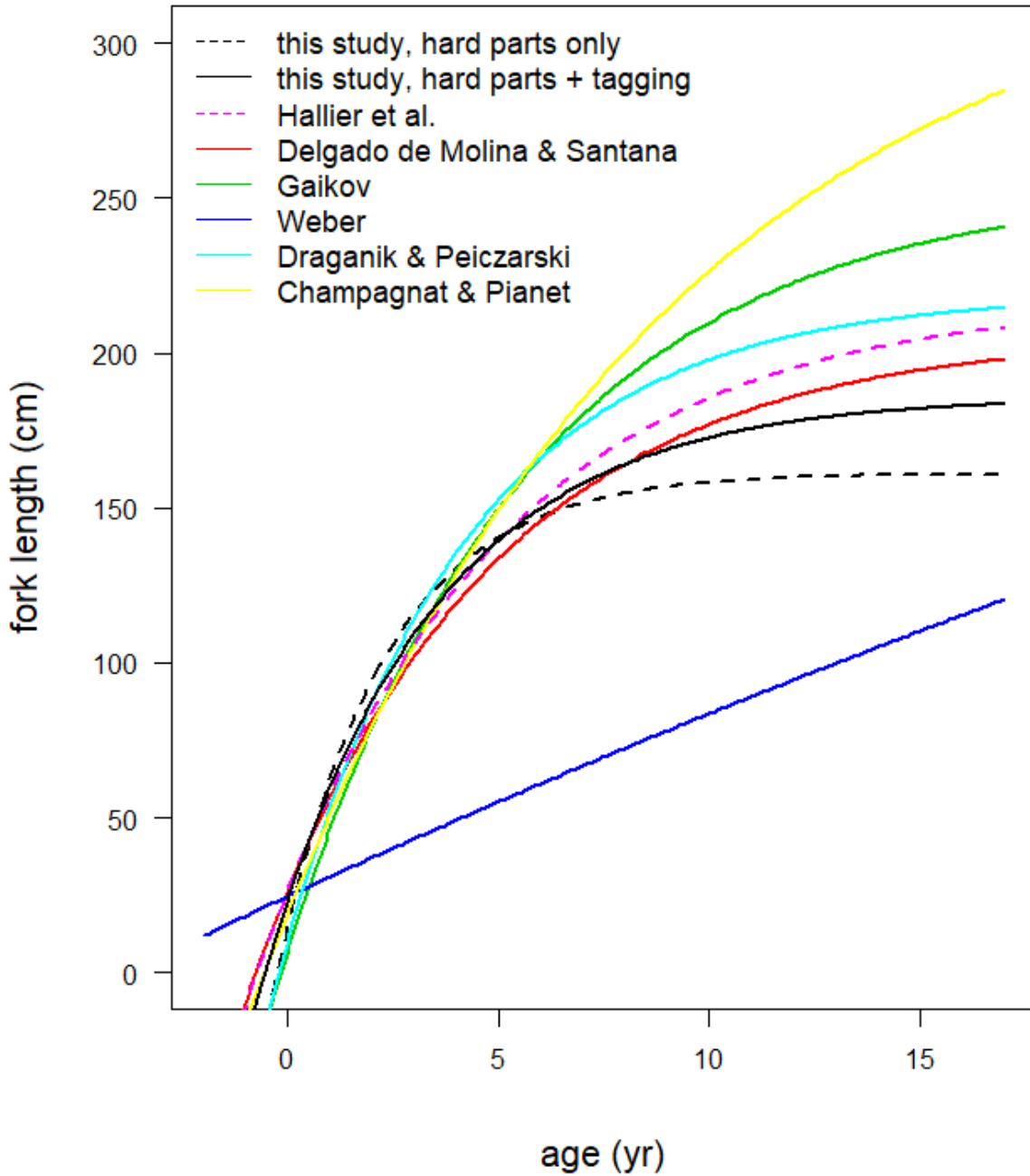
58 **Keywords:** Validated age, life history, otolith, Scombridae, growth model, tagging

59 **1. Introduction**

60 Bigeye tuna, *Thunnus obesus*, are distributed in the warm waters of the Atlantic, Pacific, and  
61 Indian Oceans where they are commercially and recreationally fished. They can grow up to 230  
62 cm in length and weigh up to 250 kg (Collette and Nauen 1983, Cayré et al. 1993). As a  
63 commercially valuable species fished in international waters by international parties, there is  
64 multi-national interest in keeping the fishery at a sustainable level. Accurately estimating the  
65 relationship between length and age provides critical information for assessment models. This  
66 paper focuses on the growth of bigeye tuna in the Atlantic Ocean.

67 Prior work for bigeye tuna in the Atlantic Ocean resulted in a variety of growth estimates, with  
68 values for the asymptotic maximum length,  $L_{\infty}$ , ranging from ~200 to ~500 cm (Figure 1,  
69 Appendix 1). These models relied on a variety of data sources to estimate growth including  
70 tagging, otoliths, spines, and length frequency data, all of which lacked old individuals and long-  
71 term tag recapture data. The 2021 International Commission for the Conservation of Atlantic  
72 Tunas (ICCAT) assessment of bigeye tuna utilized estimates from the Hallier et al. (2005)  
73 formulation of the Richards growth model, reparameterized using Schnute (1981) as required by  
74 the Stock Synthesis (SS3) assessment platform. The resulting parameters were:  $L_{\infty} = 178.6$  cm  
75 fork length (FL), the growth parameter  $K = 0.42 \text{ yr}^{-1}$  and the Richards coefficient  $p = -0.00034$   
76 (Anon. 2021).

77 *Figure 1. Comparison of estimated growth curves for bigeye tuna from the literature and the*  
78 *current study. The curve by Hallier et al. was used in the most recent stock assessment by*  
79 *ICCAT. The two curves from the current study are without the age 1 and age 2 fish in the Pelagic*



81  
82 New data collected on Atlantic bigeye tuna now allows the growth curve to be revisited. ICCAT  
83 concluded the Atlantic Ocean Tropical Tuna Tagging Programme (AOTTP) in 2021, a five-year  
84 program with the goal of tagging at least 120,000 tropical tunas with a variety of tag types (Beare

85 et al. 2019). During this time, nearly 25,000 bigeye tuna were tagged and released with just over  
86 5,000 recoveries. Around the same time, laboratories across the Atlantic worked in collaboration  
87 to develop and validate age reading protocols for the species and increase the collection of hard  
88 parts for ageing purposes.

89 A goal of this work is therefore to estimate growth of Atlantic bigeye tuna using all available  
90 data for the stock. Of particular interest was to combine multiple data sources (i.e., tagging data  
91 and otolith data, including validated ages) in order to develop the most comprehensive and up-to-  
92 date growth model for the species. This included tagging data from three different sources  
93 (AOTTP, the ICCAT historical database, and a study by Hallier et al. (2005)) and otolith data  
94 from four different sources (AOTTP, Hallier et al. (2005), and age readings from the Pelagic  
95 Fisheries Lab (PFL) and the Panama City Lab (PCL) whose protocols have been validated using  
96 bomb radiocarbon dating (Andrews et al 2020)).

97 With so many sources of information, it was clear from the outset that issues related to data  
98 quality would have to be addressed. Ailloud et al. (2014) found that ICCAT tagging data for  
99 Atlantic bluefin tuna contain useful information about growth rates if, and only if, the data are  
100 subjected to extensive quality control procedures. Such procedures have not been applied to the  
101 ICCAT bigeye tuna tagging data but have been applied to the tagging data from AOTTP (see  
102 Anon. 2021). In the present study, measurement error was estimated from short-term recapture  
103 data for the ICCAT and AOTTP tagging data as well as those of Hallier et al. (2005). It was also  
104 noted that different age reading protocols were used: Hallier et al. (2005) age estimates were  
105 based on daily growth rings while most other samples were aged using annual growth rings.  
106 While daily growth rings can provide accurate and precise age estimates in young fish, the  
107 procedure has been shown to progressively underestimate age for bigeye older than one year  
108 (Williams et al. 2013, Ailloud et al. 2019). As such, the data analysis considered several subsets  
109 of the full dataset.

110 In order to estimate growth simultaneously from tag-recapture data and otolith age-length data,  
111 the tag-recapture data must be modeled in a way that is consistent with age-length data (Francis  
112 1988a and 1988b; Laslett et al., 2002). That is, for age-length data, there is variability in length  
113 about age, so instead of modeling tag-recapture data as a function of length (i.e., using length  
114 increment data and times at liberty (Fabens 1965)) we model the lengths at release and recapture

115 while treating the unknown age at release as a random variable (Francis et al., 2016; Aires-da-  
116 Silva et al., 2015; Eveson et al. 2004; Laslett et al. 2002). This modeling approach allows for the  
117 growth information from both sources of data to be modelled as a function of age, allowing for a  
118 common set of growth parameters to be derived.

## 119 2. Methods

### 120 2.1. Tagging Data

#### 121 AOTTP Tagging Data

122 This analysis is based on AOTTP database version ‘aottp\_cisef\_20210228’. Details of the  
123 AOTTP tagging program can be found in Beare et al. (2019). In the AOTTP database there are  
124 24,252 releases of bigeye tuna (identified as bigeye in the release species code) representing  
125 24,078 unique fish. Of those tagged fish there were 5,018 recoveries (note, some of these  
126 represent fish recovered more than once from fish that were released post recovery).

127 Of the 5,018 recoveries identified as bigeye during their release, 340 were identified during  
128 recovery as yellowfin (YFT), blackfin (BLF), little tunny (LTA), or skipjack (SKJ) (Table 1).

129 *Table 1. Breakdown of species identifications during recovery of the 5,018 identified as bigeye*  
130 *during release (BET = bigeye, BLF = Bluefin, LTA = Little Tunny, SKJ = Skipjack, YFT =*  
131 *Yellowfin, UNK = unknown).*

<b>BET</b>	<b>BLF</b>	<b>LTA</b>	<b>SKJ</b>	<b>YFT</b>	<b>UNK</b>	<b>Total</b>
2,243	1	1	22	316	2,435	5,018

132

133 For the purpose of this analysis, we assume that the fish are bigeye if they were identified as  
134 bigeye during biological sampling. We also include fish that were identified as bigeye during  
135 release and recovery or bigeye during release and unknown during recovery. There are 4,678  
136 bigeye once this filter is applied (Table 2).

137 The release length type (relentype) and recovery length type (rclentype) were (straight) fork  
138 length (FL), blank, unknown (UNK), curved fork length (CFL), lower jaw to 1<sup>st</sup> dorsal (LD1),  
139 standard length (SL), or total length (TL). We retained fish which had length CFL (and  
140 converted them to FL, see Appendix 2 for details) and FL. We use the terms straight fork length  
141 and fork length interchangeably and distinct from curved fork length. There were 4,356 bigeye

142 tuna pairs left after this filter. After eliminating those fish with negative time at liberty we had  
 143 4,280 pairs. There were 4,227 remaining fish after those with missing lengths were removed;  
 144 some had times at liberty up to 150 weeks.

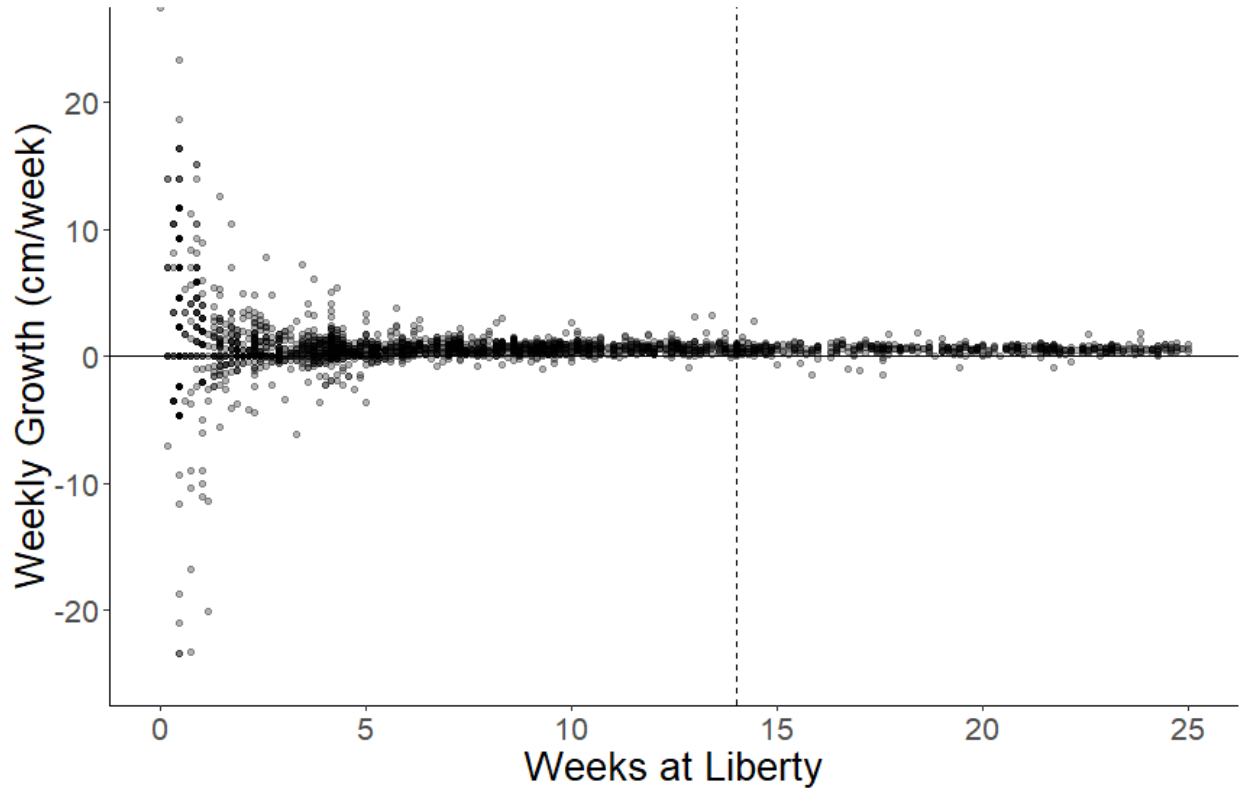
145 *Table 2. Sample size from AOTTP database for bigeye tuna data after each step in the data*  
 146 *processing to ensure only appropriate pairs of data were used in the assessment work.*

<i>Initial number of releases in database</i>	24,252
<i>Initial number of paired (release-recapture) records in the database</i>	5,018
<b>Justification for removal</b>	<b># paired records remaining</b>
<i>I – Initial data processing</i>	
Recovery length unknown or unable to convert to FL	4,678
Missing time at liberty	4,356
Time at liberty is negative	4,280
Missing release length	4,277
<i>II – Further exclusion criteria</i>	
Removed all records with time at liberty $\leq 97$ days	1,626
Removed outliers in growth	1,592

147  
 148 Over short times at liberty the observed growth increments largely represent measurement error  
 149 rather than somatic growth (Ailloud et al. 2014). We examined the distribution of unreasonable  
 150 growth increments (negative weekly growth) as a function of time at liberty to determine a  
 151 threshold time at liberty at which measurement errors are minimal while retaining as great a  
 152 sample size as possible. In order to match what was done across other datasets, 98 days was used  
 153 as the cutoff for determining the time at liberty that represents real growth rather than  
 154 measurement error. This left 1,626 records (Table 2). In an attempt to eliminate outliers due to  
 155 data entry and measurement errors, we removed records with the fastest and slowest 1% absolute  
 156 growth per day (i.e., below the 0.01 and greater than the 0.99 quantiles). This resulted in 1,592  
 157 records for analysis.

158 *Figure 2. Plot of weekly growth (cm/week) versus time at liberty (weeks) based on straight fork*  
 159 *length (FL) measurements at time of tagging and recapture from 4,256 bigeye tuna in the*  
 160 *AOTTP database. Only records for fish at liberty for up to 25 weeks are shown (maximum time*  
 161 *at liberty is 161 weeks). The dashed vertical line is at 98 days. Due to the amount of data the*  
 162 *circles have been made slightly transparent; circles that appear black (rather than grey) indicate*  
 163 *multiple data points at this value.*

164

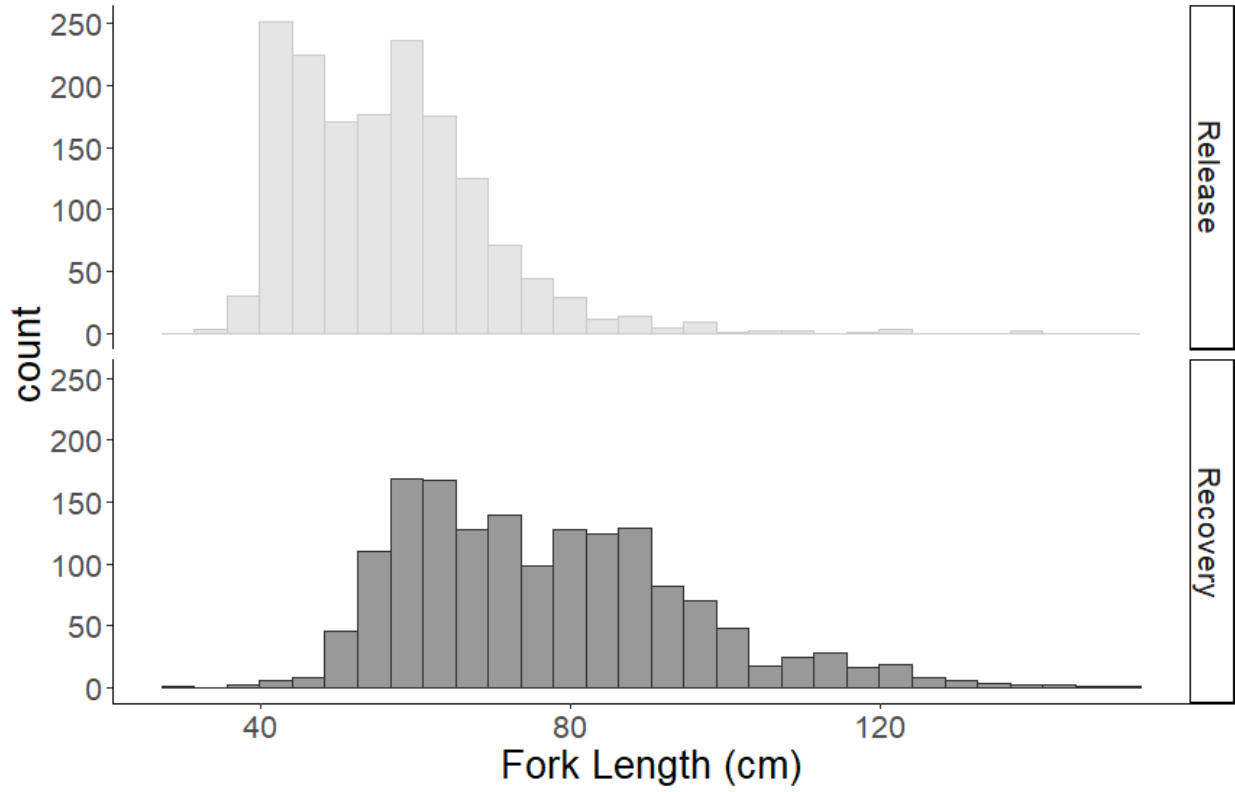


165

166 The resulting dataset for bigeye consisted of 1,592 records with lengths at tagging ranging from  
 167 33 cm FL to 140 cm FL, lengths at recapture ranging from 28 cm FL to 150 cm FL (Figure 3)  
 168 and times at liberty ranging from 98 to 1,127 days (median= 239 days). The releases peaked in  
 169 March and then July to November, while the majority of the recoveries occurred May to August  
 170 with a peak in July (Figure 4).

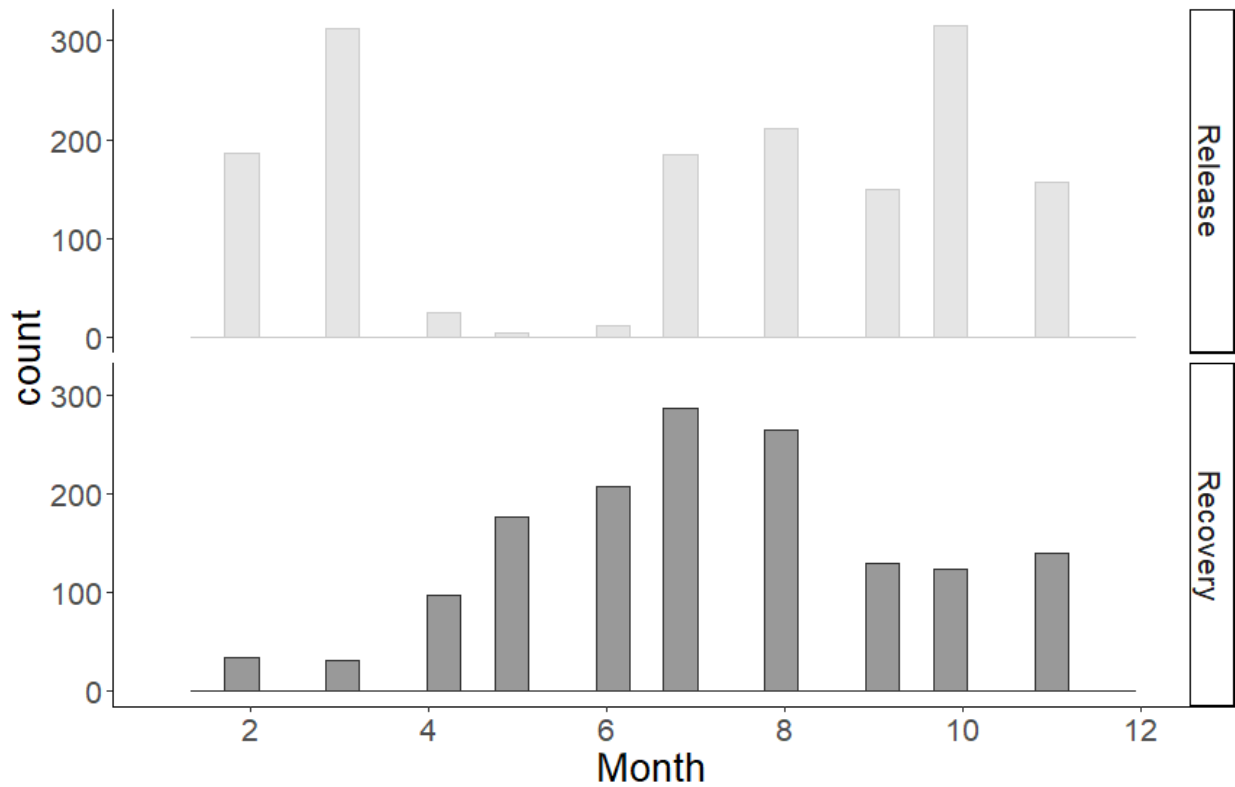
171 *Figure 3. Histogram of lengths (cm) for the 1,592 bigeye tuna used in this analysis at release*  
 172 *(top) and recovery (bottom) from the AOTTP database.*





173

174 *Figure 4. Histogram of month of release (top) and recovery (bottom) for the 1,592 bigeye tuna*  
 175 *from the AOTTP database used in this analysis.*



176

177 *ICCAT Tagging Data*

178 The ICCAT tagging database (ICCAT Secretariat n.d.) begins in 1960 for bigeye tuna and has  
 179 releases or recaptures for 54 years (through 2020, which overlaps with the AOTTP tagging  
 180 program). The tagging database has a total of 35,462 releases and 7,996 recoveries, although  
 181 many of these (24,212 releases and 5,115 recoveries) are part of the AOTTP database (Table  
 182 3). A further 55 records have unknown release years and 115 records had missing recovery  
 183 years. There are 2,108 pairs of release and recoveries with known dates of release and recovery  
 184 and known lengths at release and recovery.

185 Of the 2,108 pairs of release/recovery, only 45 had both pairs with known measurement unit  
 186 (either FL or LJF), and the rest were unknown. We treated LJF (lower jaw fork length) as  
 187 equivalent to FL and thus all 45 lengths were retained. After removing those fish with negative  
 188 time at liberty we had 44 pairs.

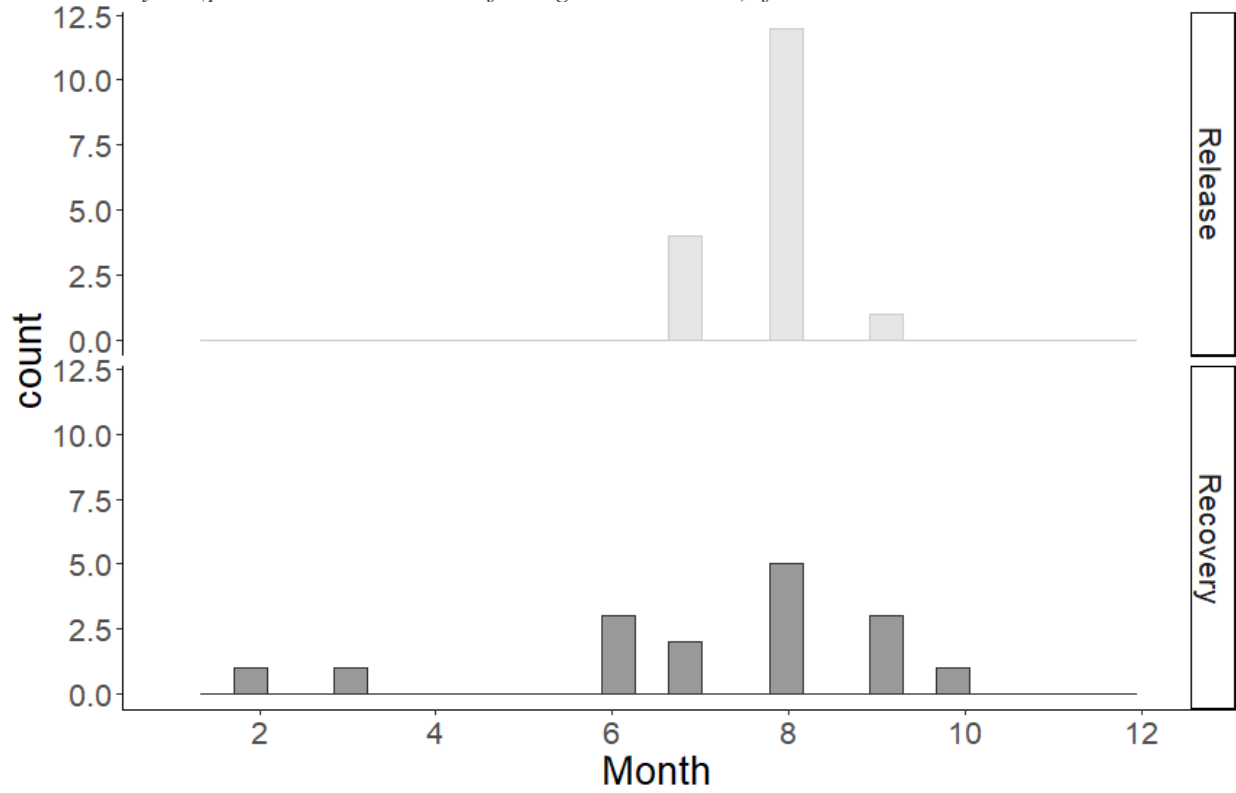
189 *Table 3. Sample size from ICCAT database for bigeye Tuna data after each step in the data*  
 190 *processing to ensure only appropriate pairs of data were used in the assessment work.*

<i>Initial number of releases in database</i>	35,462
<i>Initial number of paired (release-recapture) records in the database</i>	7,996
<b>Justification for removal</b>	<b># paired records remaining</b>
<i>I – Initial data processing</i>	
Part of AOTTP database	2,881
Recovery date is missing	2,826
Release date is missing	2,826
Release or recovery length is unknown	2,108
Release or recovery measurement unit (e.g., FL or LJF) is unknown	45
Time at liberty is negative	44
<i>II – Further exclusion criteria</i>	
Removed all records with time at liberty $\leq 97$ days	19
Removed any record that could overlap with Hallier	18
Removed growth outlier	17

191

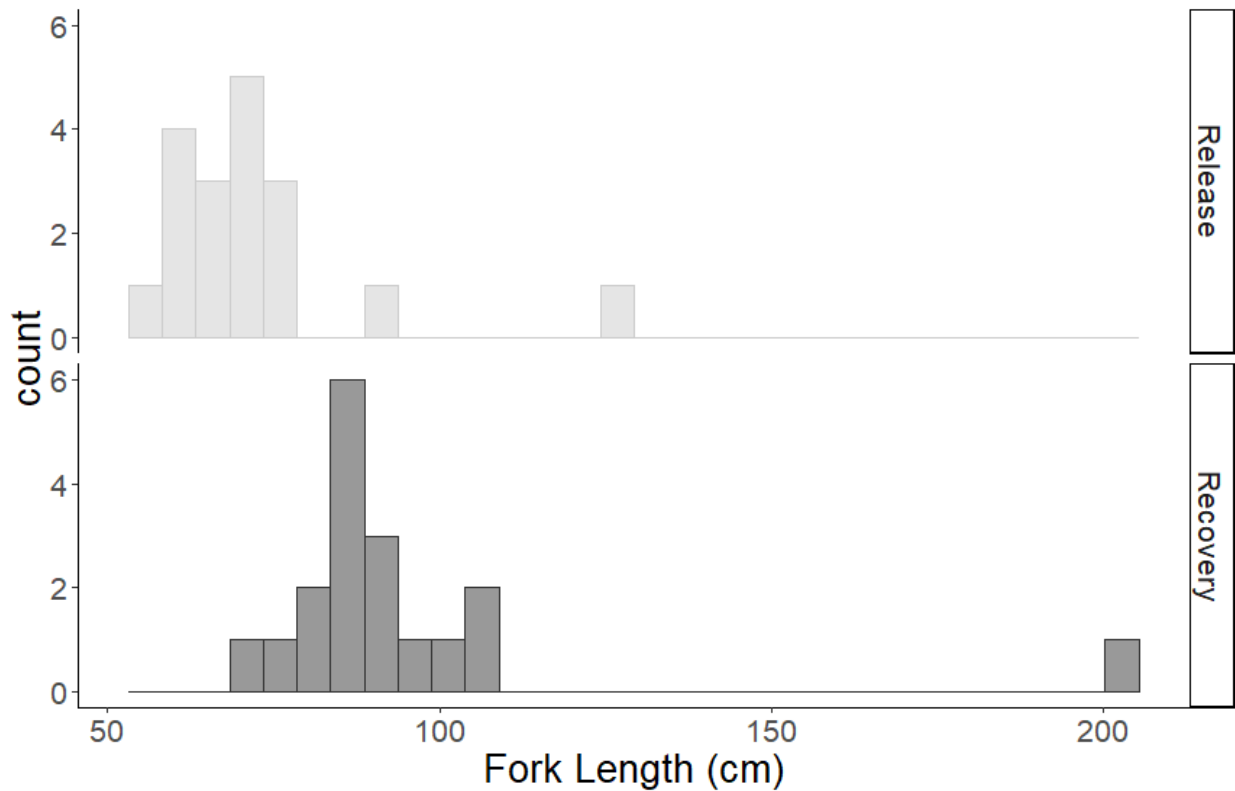
192 The majority of the tagged bigeye from the ICCAT database were tagged in the months of July  
 193 and August with recoveries throughout the year, but with a peak in August (Figure 5). The  
 194 release FL ranged from 56 to 129 cm and the recovery FL ranged from 12.5 to 203 cm (Figure  
 195 6).

196 *Figure 5. Histogram of month of release (top) and recovery (bottom) for the 18 bigeye tuna used*  
 197 *in this analysis (prior to the removal of the growth outlier), from the ICCAT database.*



198  
 199 *Figure 6. Histogram of lengths (cm) for the 18 bigeye tuna used in this analysis at release (top)*  
 200 *and recovery (bottom) from the ICCAT database. The fish with recovery length of 203 cm is an*

201 *apparent outlier and was discarded (see Figure 10).*

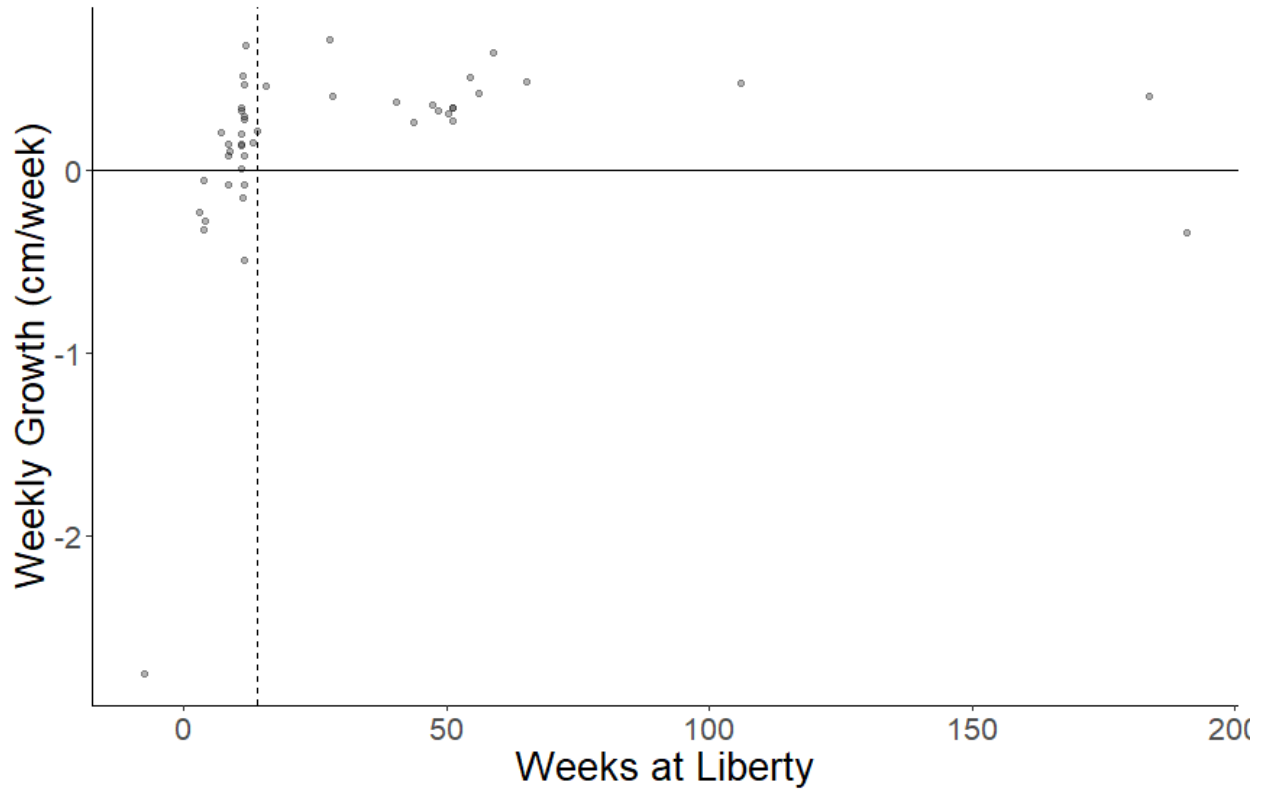


202

203

204 In order to avoid including records where observed growth rates most likely reflect measurement  
205 error or tagging effects, only data for fish at liberty >97 days were retained, leaving 19 data pairs  
206 to analyze (Figure 7). Of these 19 pairs, 16 had lengths that were measured at both release and  
207 recovery; 2 pairs had unknown (either estimated or measured) measurement type at release and  
208 recovery; and 1 pair had estimated measurement type at release and unknown at recovery. One  
209 additional record was removed to avoid overlapping with the Hallier et al. (2005) data (discussed  
210 below), as those data occur in the ICCAT database, but we were unable to uniquely identify the  
211 records. The one removal was a release from 2000 and this overlaps with the time frame of the  
212 Hallier data (releases in 1994 to 2000). Another record has an unreasonable growth trajectory  
213 (see Figure 10) and was removed. This resulted in 17 usable records from the ICCAT database.

214 *Figure 7. Growth per week (recorded growth divided by weeks at liberty) versus time at liberty*  
215 *for bigeye tuna from the ICCAT database. The dashed vertical line denotes the 98 day time at*  
216 *liberty cutoff used in this study.*

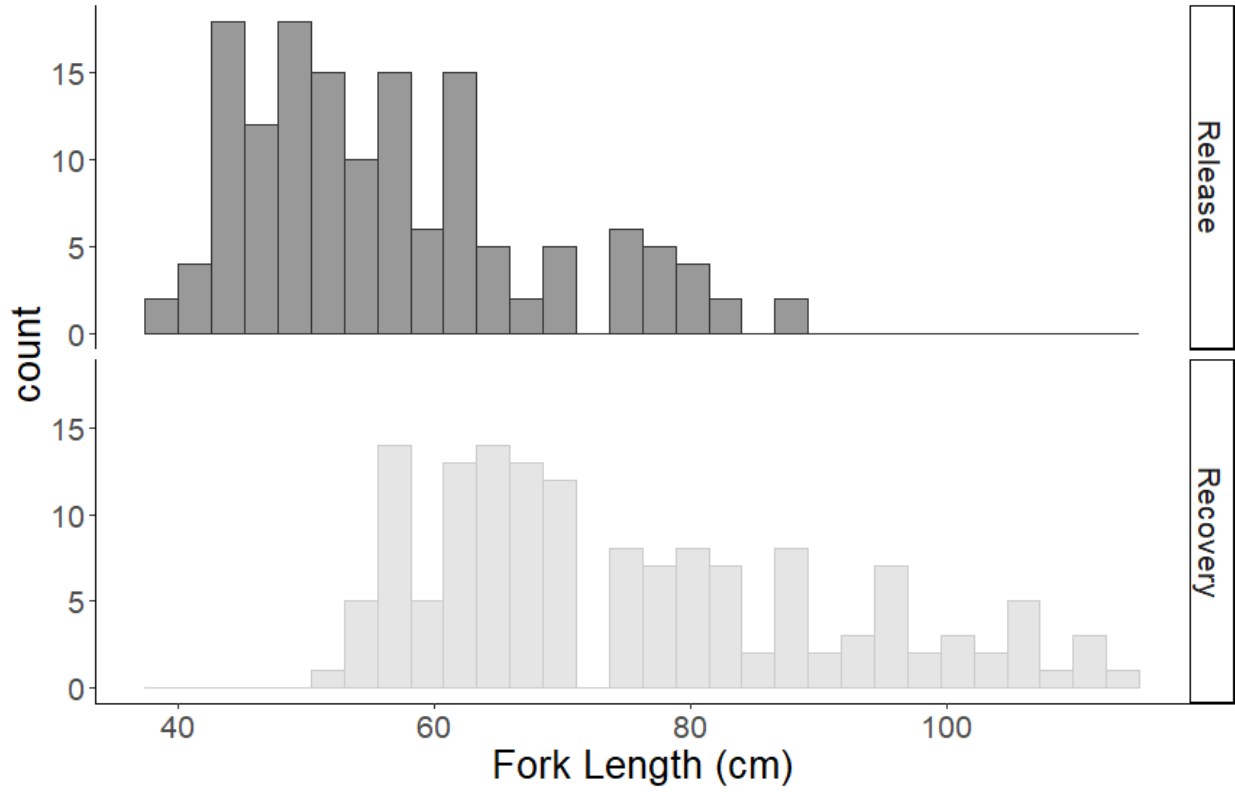


217  
218

219 *Tagging Data from Hallier et al. (2005)*

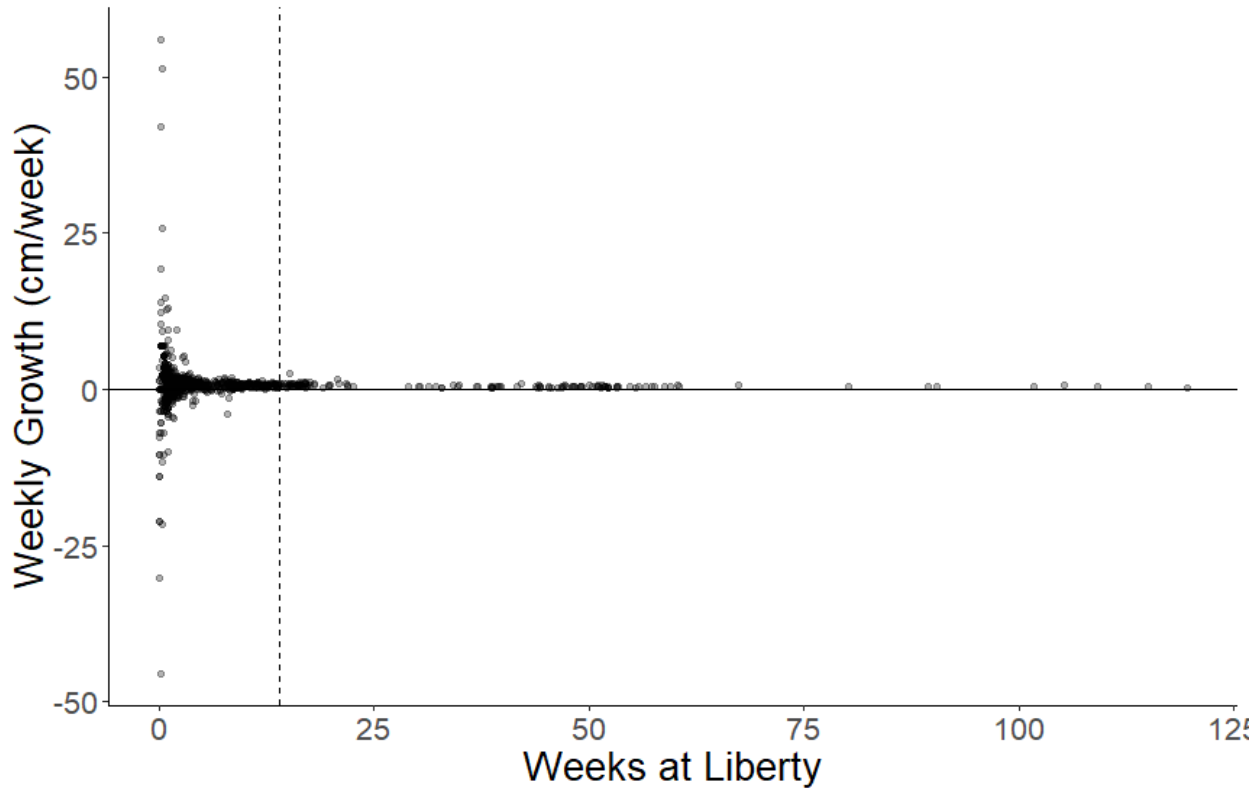
220 We obtained data from a previous study in the eastern Atlantic Ocean (Hallier et al. 2005) that  
 221 included 625 bigeye tagged and recaptured with FL ranging from 37 to 124 cm (Figure 8). When  
 222 98 days is used as the time at liberty cutoff (to be consistent with AOTTP and ICCAT tagging  
 223 data), 146 bigeye release and recoveries remain (Figure 9). Originally Hallier used 14 days as the  
 224 cutoff.

225 *Figure 8. Frequency of recovery fork lengths (cm), top panel, and release lengths (cm), bottom*  
 226 *panel, for bigeye tuna from the tagging data of Hallier et al.*



227

228 *Figure 9. Growth per week (recorded growth divided by weeks at liberty) versus time at liberty*  
 229 *for bigeye tuna from the tagging data of Hallier et al. The dashed vertical line denotes the 98*  
 230 *day time at liberty cutoff used in this study.*



231

232 *2.2. Otolith data*

233 The otolith data comprised samples aged using two different reading protocols: one based on  
 234 daily increment counts and the other on annual ring counts. Results from blind counts of micro-  
 235 increments in chemically marked bigeye tuna have found that micro-increment counts tend to  
 236 underestimate true times at liberty (Ailloud et al. 2019; Farley et al. 2020), indicating that daily  
 237 counts are likely to underestimate true age. Additional work by Williams et al. (2013) has shown  
 238 that age counts of presumed daily growth increments can lead to an underestimation of age in  
 239 fish older than 1 year (Williams et al., 2013). As such, for all hard part data utilized in this  
 240 analysis, daily readings were restricted to bigeye less than 1 year of age. The ageing protocol  
 241 based on annual ring counts (Allman et al. 2020) that was used for all samples described below  
 242 has been validated through bomb radiocarbon dating (Andrews et al. 2020) and preliminary  
 243 results from AOTTP fish marked with oxytetracycline support the hypothesis that the larger  
 244 growth increments are deposited on an annual basis (Ailloud et al. 2019).

245 *AOTTP Otolith Data*

246 A total of 63 pairs of otolith age and length was obtained through the AOTTP from fish sampled  
247 across a large area of the Atlantic Ocean. Twenty-six of those samples were read by a single  
248 expert using annual growth increment counts, while the remaining 37 (the ‘reference collection’)  
249 were aged by three independent readers who counted daily rings (Figure 10; Beare et al. 2019).

250 Whole otoliths were imaged and weighed prior to processing. Each core was marked prior to  
251 embedding in embedding in polyplex clear ortho casting resin (Allnex<sup>®</sup>). Transverse sections  
252 were cut through the center of each otolith using an Isomet 1000 low-speed saw with diamond  
253 edged wafering blades. Sections were then mounted on microscope slides (76.2 x 25.4mm) using  
254 thermoplastic resin (Cystalbond 509 <sup>©</sup>) with the side of the section furthest away from the core  
255 facing up. Each section was ground to a thickness between 320 – 350  $\mu\text{m}$  using wet/dry  
256 sandpaper (800 and 1200 grit), lubricated with distilled water. A small drop of microscope  
257 immersion oil (Cargille <sup>©</sup> -TYPE A) was added prior to imaging to help clear up the ground  
258 surface of the otolith and aid in the imaging process.

259 Otolith sections were imaged under transmitted light. Annual ages were assigned to individuals  
260 based on the number of fully formed opaque zones (i.e., presence of translucent otolith material  
261 between the outer edge of the last opaque zone and the otolith margin). All age readings were  
262 made without knowledge of fish size, otolith weight, sex, location of capture or time at liberty.  
263 Methods for the annual age reading followed those developed for other tuna species (Farley et  
264 al., 2013, 2006; Gunn et al., 2008; Lang et al., 2017). Ageing protocols developed for Atlantic  
265 bluefin tuna (Neilson and Campana, 2008; Rodríguez-Marín et al., 2014, 2007; Secor et al.,  
266 2014) were also used as a basis to aid interpretation of what may constitute an annual growth  
267 zone in Atlantic tunas.

268 Micro-increment counts were conducted at various magnifications ranging between 400 and  
269 1000x. The method for the interpretation of the microstructure was consistent with those  
270 methods published for reading transverse sections (Lehodey and Leroy, 1999; Sardenne et al.,  
271 2015; Shuford et al., 2007). After a count of between 150-180 the internal micro-structure  
272 becomes increasingly difficult to interpret. For subsections of the otolith where increments were  
273 either difficult to interpret or not present, an interpolation method based on the zone pattern  
274 immediately before and after the difficult area was applied.

275 *2.1.5. Otolith Data from Pelagic Fisheries Lab*



276 A total of 229 sets of otoliths was extracted from bigeye tuna landed by commercial pelagic  
277 longline vessels and recreational rod and reel fisheries along the east coast of the United States  
278 between June and November of 2018-2020. Catch locations include the Gulf Stream, along the  
279 continental shelf, and slope canyons from Cape Hatteras to the Hague Line. FL (cm) of  
280 individuals sampled from recreational fisheries and CFL from commercial longline fisheries  
281 were recorded. To standardize length across gears tunas measured in CFL were converted to FL  
282 using a regression equation developed by Farley et al. (2006). Fish ranged in size from 69.7 to  
283 174.7 cm SFL. The minimum length in US waters for bigeye is 27 inches (68.58 cm) curved fork  
284 length, resulting in only large age 1 and 2 fish being retained. After extraction, sagittal otoliths  
285 were rinsed with water, dried, and stored in vials.

286 Otolith processing was based on methods developed by Busawon et al. (2015) and modified by  
287 Rodrigues-Marin (2019) for Atlantic bluefin tuna (*Thunnus thynnus*). All otoliths were cleaned  
288 in a jewelry sonicator to remove any remaining residual tissue that dried after extraction. Whole  
289 sagittal otoliths (left and right) were weighed and imaged, then embedded using Epothin 2 Epoxy  
290 hardener and resin at a 17:40 ratio respectively. Transverse sections were cut using an Isomet  
291 1000 low-speed saw with diamond edged Buehler blades. Four transverse sections, 0.8 mm in  
292 width, were cut beginning with a rostral 'V-section' that included the origin.

293 Sections were mounted to glass slides using *QuickStick* Mounting Wax with the side closest to  
294 the origin facing down. After mounting, sections were polished using 180, 320 and 600 grit  
295 sandpaper to a width of roughly 0.3-0.5mm. A final polish with a felt pad containing a light  
296 coating of water mixed with *MicroPolish 2* Alumina powder was applied to each section. Otolith  
297 sections were imaged under transmitted light with a compound microscope and features such as  
298 contrast and brightness were adjusted for each section in Adobe Photoshop. A 1mm scale bar  
299 was created and placed at the first inflection point on the ventral arm of each bigeye section  
300 image to provide the reader guidance on the approximate location of first annulus formation  
301 based on mean distances in Farley et al. (2006).

302 All four sections were read twice by the same reader with no *a priori* information about the  
303 section (e.g., fish size, weight, previous age estimates). After analysis, only the two sections  
304 closest to the origin were used for age final estimation and reading error estimates. If age  
305 estimates from the first and second read were not identical, the section was aged again and

306 assigned a final age based on that third reading. A readability score on a scale from 1-5 (1 =  
307 unreadable, 5 = excellent) was established and sections with low readability scores (mean score  
308  $\leq 2.5$ ) were not included in final age estimates. Annual ages were assigned to individuals based  
309 on the number of fully formed opaque zones.

#### 310 *2.1.6. Otolith Data from Hallier et al. (2005) (Daily readings)*

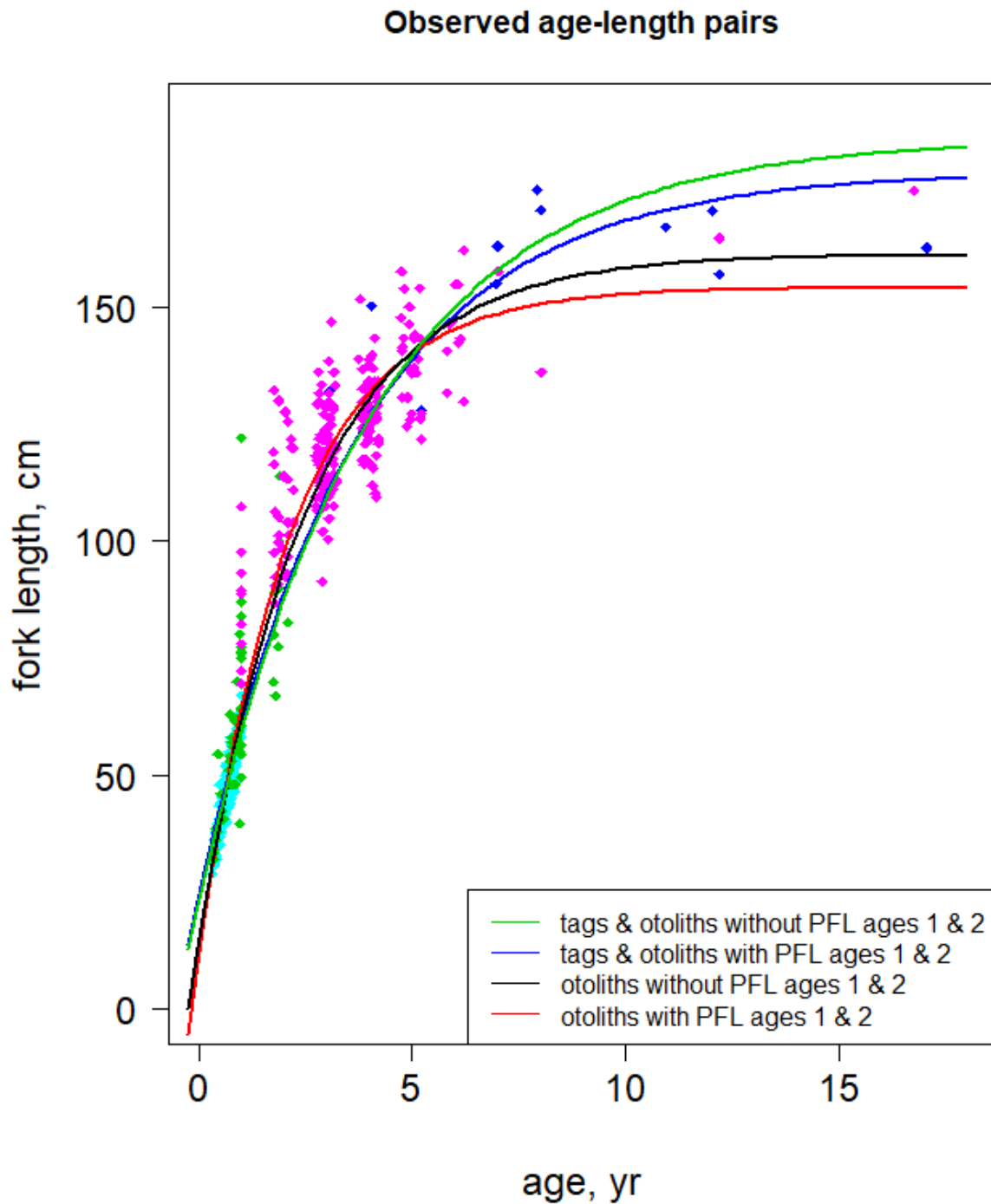
311 Data from a 2005 study published by Hallier included 255 bigeye tuna otoliths read for daily age  
312 (Hallier et al. 2005). The lengths ranged from 20 to 190 cm (FL) and the ages (in days) ranged  
313 from 116 to 3,324. A light microscope was used for readings from fish with FL less than 74 cm  
314 and a scanning electron microscope for fish with FL equal to or bigger than 74 cm. The otolith  
315 preparation and reading protocols are described in detail in Hallier et al. (2005). Hallier's  
316 original study retained 83 of the 108 otoliths from Dakar, Senegal, and 147 from Abidjan, Ivory  
317 Coast. Given concerns regarding potential underaging of fish, in the current study the dataset was  
318 restricted to 153 age-length pairs from fish under 1 year old (Figure 10). Fork lengths for this  
319 subset ranged from 29 to 67 cm.

#### 320 *2.1.7. Otolith Data from the Panama City Lab*

321 Twelve otoliths prepared and read by the Panama City Lab (PCL) were included in this study.  
322 Detailed protocols are described in Pacicco et al. (2021) and are aligned with the  
323 abovementioned annual ageing protocols (Allman et al. 2020). Ages determined by counting  
324 purported annual growth zones in these twelve Bigeye otolith cross sections were validated with  
325 bomb radiocarbon dating (Andrews et al 2020). The valid age-at-length data for Bigeye were 3–  
326 17 years for fish lengths of 128.0–175.0 cm FL (n = 12) (Figure 10).

327

328 *Figure 10. Plot of all the length-age pair data (excluding fish greater than one year of age in the*  
329 *dataset of Hallier et al. (2005)). Blue symbols represent data from Panama City Lab; cyan =*  
330 *ages from daily ring counts by Hallier et al. (2005), green symbols = AOTTP readings of annual*  
331 *rings in otoliths, magenta = data from Pelagic Fisheries Lab (PFL). Integer ages >1 have been*  
332 *jittered to reduce overprinting. Four fitted von Bertalanffy curves are shown which differ in*  
333 *whether age 1 and age 2 fish from the PFL dataset are included and whether tagging data is*  
334 *used in addition to the otolith data.*



335

336 *2.2. Growth Curve Analyses*

337 We fitted two different growth models to the tag-recapture data and counts of growth rings in  
 338 otoliths: the Richards and the von Bertalanffy models. The Schnute (1981) parameterization was

339 used as it allows for both models to be expressed using a single equation where the shape  
 340 parameter,  $p$ , controls the level of curvature and reverts the function to a classic von Bertalanffy  
 341 model when  $p$  is equal to 1.0.

342 All computations (except for the integrated analyses) were done using the R program language  
 343 (R Core Team 2020). Models based on just the otolith data were fitted using the R package  
 344 ‘FSA’ (Ogle et al. 2020). For the integrated analyses, we used the “Aires da Silva-Maunders-  
 345 Schaefer-Fuller with correlation” (AMSFc) framework (Francis et al. 2016). This approach  
 346 models the release and recapture lengths of fish as functions of age by treating age at tagging as a  
 347 random effect. It also accounts for correlation between the measurements of an individual  
 348 through the parameter  $\rho$ , which models correlation as a simple decreasing function of time  
 349 at liberty ( $\Delta t$ ; Francis et al. 2016). The objective function is the sum of the bivariate normal  
 350 log-likelihood of the release and recapture lengths, the lognormal log-likelihood of the random  
 351 effects and the log-likelihood of the otolith data. Computer code in AD Model Builder (Fournier,  
 352 D.A. et al. 2012) was used that was based on the Bluefin tuna work of Ailloud et al. (2017).

353 For the Schnute (1981) model, the following equations are used:

$$354 \quad L_a = \left( (L_1)^p + ((L_2)^p - (L_1)^p) \frac{(1 - \exp(-K(a - A_1)))^{\frac{1}{p}}}{(1 - \exp(-K(A_2 - A_1)))^{\frac{1}{p}}} \right)^{\frac{1}{p}} \quad \text{(Equation 1)}$$

$$355 \quad L_{a+\Delta t} = \left( (L_1)^p + ((L_2)^p - (L_1)^p) \frac{(1 - \exp(-K(a + \Delta t - A_1)))^{\frac{1}{p}}}{(1 - \exp(-K(A_2 - A_1)))^{\frac{1}{p}}} \right)^{\frac{1}{p}} \quad \text{(Equation 2)}$$

$$356 \quad L_\infty = \left( \frac{\exp(KA_2)(L_2)^p - \exp(KA_1)(L_1)^p}{\exp(KA_2) - \exp(KA_1)} \right)^{\frac{1}{p}} \quad \text{(Equation 3)}$$

$$357 \quad t_\theta = A_1 + A_2 - \frac{1}{K} \ln \left( \frac{\exp(KA_2)(L_2)^p - \exp(KA_1)(L_1)^p}{(L_2)^p - (L_1)^p} \right) \quad \text{(Equation 4)}$$

$$358 \quad t^* = A_1 + A_2 - \frac{1}{K} \ln \left( p \frac{\exp(KA_2)(L_2)^p - \exp(KA_1)(L_1)^p}{(L_2)^p - (L_1)^p} \right) \quad \text{(Equation 5)}$$

359 where:

360  $a$  is age,

361  $L_a$  is the expected length of a fish of age  $a$ , thus  $L_{a+\Delta t}$  is the expected length of a fish tagged at  
 362 age  $a$  and recaptured at age  $a + \Delta t$ ,

363  $L_\infty$  is the asymptotic length,

364  $K$  is the growth coefficient,  
 365  $t_0$  is the theoretical age at size 0 in the von Bertalanffy growth model ( $p = 1$ ),  
 366  $t^*$  is age at which the inflection of the Richards growth curve occurs ( $p \neq 0$ ),  
 367  $A_1$  is age of youngest fish in sample,  
 368  $A_2$  is age of oldest fish in sample,  
 369  $L_1$  is the expected length of fish age  $A_1$ ,  
 370  $L_2$  is the expected length of fish age  $A_2$ .  
 371

372 In fitting the model, there are three types of parameters: those fixed by the user ( $A_1$  and  $A_2$ ), those  
 373 estimated when maximizing the likelihood ( $L_1$ ,  $L_2$ , and the parameters defining the error structure  
 374 (see below)), and those derived from the other parameters ( $L_\infty$ ,  $t_0$ , and  $t^*$  (see above) and  $a^*$  and  
 375  $b^*$  (see below)). The parameters of the error structure are:

376  $k_\rho$  steepness of slope ( $k_\rho > 0$ ) defining relationship between correlation coefficient ( $\rho$ ) and time  
 377 at liberty (higher value means the faster the correlation coefficient declines to zero),

378  $\rho_0$  correlation ( $\rho$ ) between length at tagging and length at recovery when time at liberty is zero  
 379 ( $0 < \rho_0 < 1$ , and note that  $\rho = 1 - \frac{1-\rho_0}{1-\rho_0-\rho_0 e^{(-k_\rho \Delta t)}}$  where  $\Delta t$  is time at liberty),

380  $\sigma_{L_1}$  variability in length for fish at age  $A_1$ ,

381  $\sigma_{L_2}$  variability in length for fish at age  $A_2$ ,

382  $\mu_{\log A_{tag}}$  - mean for random effects for age at tagging (follows lognormal distribution),

383  $\sigma_{\log A_{tag}}$  - standard deviation for random effects for age at tagging (follows lognormal  
 384 distribution),

385

386 The derived parameters are:

387  $a^*$  intercept for true variability around mean curve (variability in length at age) - linear model,

388  $b^*$  slope for true variability around mean curve (variability in length at age) - linear model, (note -

389  $\sigma_{L_a} = a^* + b^*$ ).

390

391 When  $p = 1$ , the model reverts to a von Bertalanffy model. Otherwise, the model assumes a  
392 Richards form.

393

### 394 2.3. Measurement Error

395 It is possible to estimate the measurement error from short-term recaptures for fish with  
396 measured or estimated lengths (Ailloud et al. 2014). Define an increment,  $I$ , to be the length at  
397 the time of recapture,  $L_r$ , minus the length at the time of tagging,  $L_t$ . Over a suitably short time at  
398 liberty, the expected value of an increment is zero. We assume growth for any fish at liberty for  
399 less than  $\Delta$  days is zero, the two recorded lengths are determined independently, the  
400 measurement error is the same at the time of tagging and recapture, and it does not vary with the  
401 length of the fish. Then the variance of the increments is

$$402 \quad \text{Var}(I) = \text{Var}(L_r - L_t) = \text{Var}(L_r) + \text{Var}(L_t) = 2\sigma^2 \quad (\text{Equation 6})$$

403 where  $\text{Var}(L_r)$  and  $\text{Var}(L_t)$  refer to the variance of repeated measurements of the same fish and is  
404 the measurement error. Hence, the measurement error standard deviation can be estimated by  
405 dividing the increment standard deviation by the square root of 2. If  $\Delta$  is a short period of time,  
406 there is high assurance that growth while at liberty is close to zero at the cost of a smaller sample  
407 size compared to using a larger  $\Delta$ . We Use  $\Delta = 25, 50, 75$  and 98 days.

## 408 3. Results

### 409 3.1. Length measurement error

410 The Hallier et al. (2005) data have the lowest measurement error for length (4.7 or 4.9 cm  
411 depending on whether the cutoff  $\Delta$  is set to 25 or 50 days) based on more than 500 paired  
412 measurements. The AOTTP data have slightly higher but similar measurement error (6.8 cm for  
413 both 25- and 50-day cutoffs, based on more than 900 paired measurements). The ICCAT  
414 database is extensive but there are very few short-term recaptures. With a cutoff  $\Delta$  of 50 days,  
415 there are only 5 measurement pairs. With the 98-day cutoff, there are 26 pairs and the estimated  
416 measurement error is 10.9 cm. However, the mean size of the tagged fish increased by about 2  
417 cm while at liberty so some of the estimated measurement error might be due to unaccounted  
418 growth. With such a small sample size, this estimate is sensitive to outliers and the removal of a  
419 single datapoint reduces the estimated measurement error to 3.9 cm.

420

421 **3.2. Growth Curves Fitted to Otolith Data**

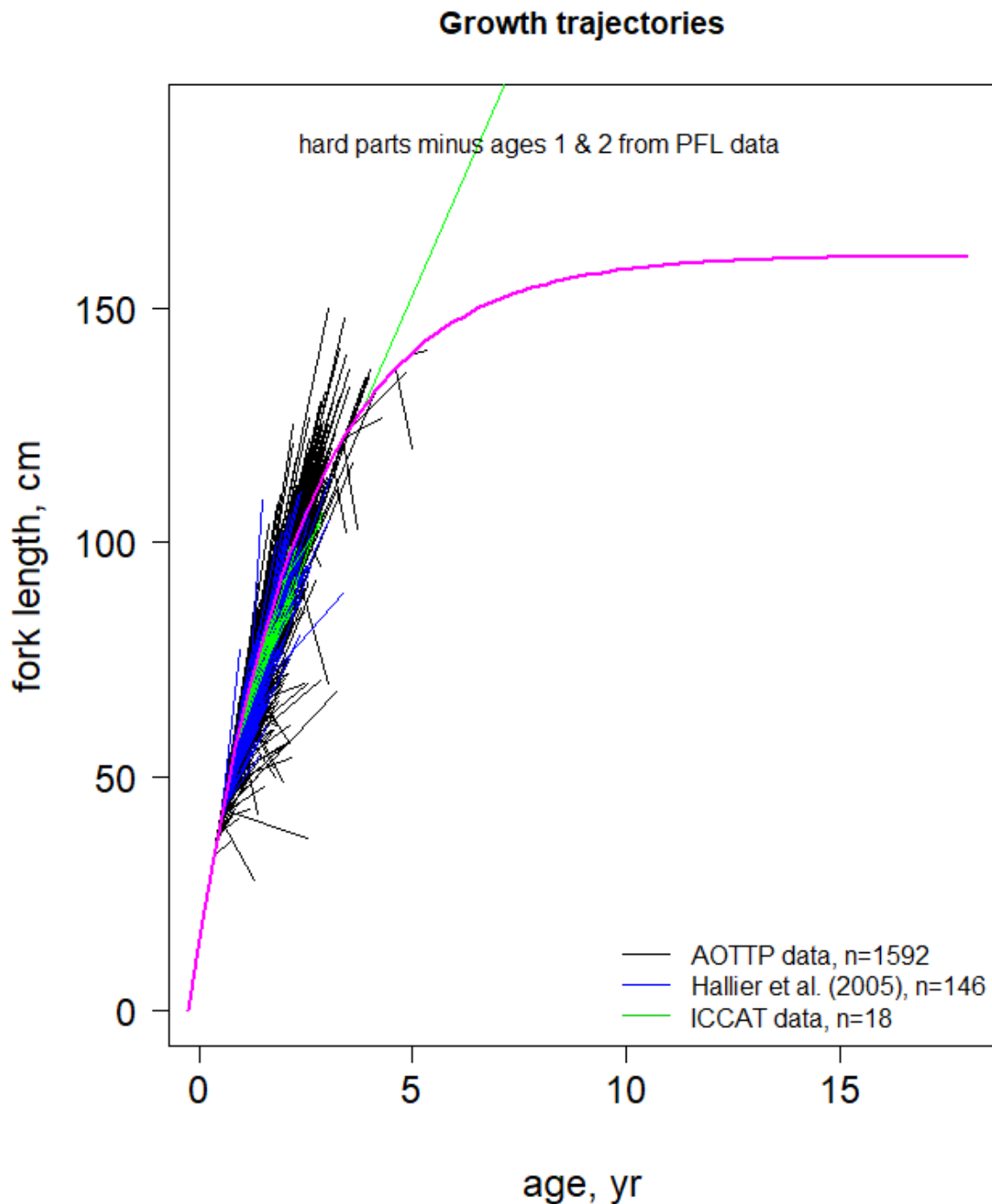
422 The nonlinear least squares estimates for models fitted to just otolith data are given in Table 4  
 423 along with non-parametric bootstrap estimates from 999 resampled datasets using the package  
 424 ‘nlstools’ (Baty et al. 2015). Goodness of fit of the von Bertalanffy growth model can be judged  
 425 from Figure 10. The otoliths for the six oldest fish, four from the PCL data and two from the PFL  
 426 data, are above the fitted growth curve when age-1 and age-2 fish from the PFL data are included  
 427 in the study (red line). A sensitivity analysis was conducted on the influence of age-1 and age-2  
 428 fish from the PFL dataset. Those age-1 and age-2 fish had larger lengths than other age-1 and  
 429 age-2 fish, indicating a potential sampling bias. All of the age-1 and age-2 fish from the PFL data  
 430 were removed from the analysis (n=41). Once these data points were removed the von  
 431 Bertalanffy model was refit to the length-age pair data (Table 4, Figure 10). The removal of the  
 432 large age-1 and age-2 fish caused the estimate of asymptotic length to increase, the estimate of  
 433 the time-axis intercept to decrease, and the estimate of  $K$  to decrease. When the larger age-1 and  
 434 age-2 fish are removed, five of the oldest fish fall above the line and one below (Figure 10, black  
 435 line). Because the number of old fish in the dataset is limited, we fit the von Bertalanffy model  
 436 while fixing the value of  $L_{\infty}$  (between 145 and 200) to provide plausible pairs of  $K$  and  $L_{\infty}$  for  
 437 use in population models (see Table 1 of Appendix 5).

438 *Table 4. Parameter estimates from fitting von Bertalanffy models to the otolith data and also the*  
 439 *von Bertalanffy results from the integrated model applied to the otolith and tagging data. Also*  
 440 *shown are the parameter estimates when age-1 and age-2 fish were removed from the PFL*  
 441 *otolith data for both models. The 95% Bootstrap confidence interval is given in parentheses for*  
 442 *the parameter estimates from the otolith data only model. The standard deviation is given in*  
 443 *parenthesis for the parameter estimates from the otolith and tagging data.*

Parameter	Otolith Data only		Integrated Model, Otolith data + Tagging	
	All otoliths	PFL age 1 and 2 otoliths removed	All otoliths and tagging data	PFL age 1 and 2 otoliths removed and tagging data
$K$	0.464 (0.403, 0.543)	0.392 (0.355, 0.441)	0.271 (0.015)	0.252 (0.014)
$L_{\infty}$	154.148 (147.081, 161.491)	161.206 (154.389, 166.835)	178.700 (5.906)	185.780 (6.298)
$t_0$	-0.163 (-0.250, -0.085)	-0.239 (-0.306, -0.175)	-0.537 (0.028)	-0.524 (0.025)

444

445 Figure 11a. Vector plot of the tagging data from AOTTP, Hallier et al. (2005) and ICCAT. The vector  
446 plot is made by computing the predicted age for the length at tagging using the estimated von Bertalanffy  
447 growth parameters, and then assuming the age at recapture is the predicted age at tagging plus the time  
448 at liberty. The von Bertalanffy curve is based on the growth model from the otolith data only without the  
449 data for age-1 and age-2 fish from the PFL dataset. The fastest growing 1% and the slowest growing 1%  
450 (in cm/wk) of the records have been eliminated from the AOTTP data. One obvious outlier is seen among  
451 the 18 records from ICCAT.

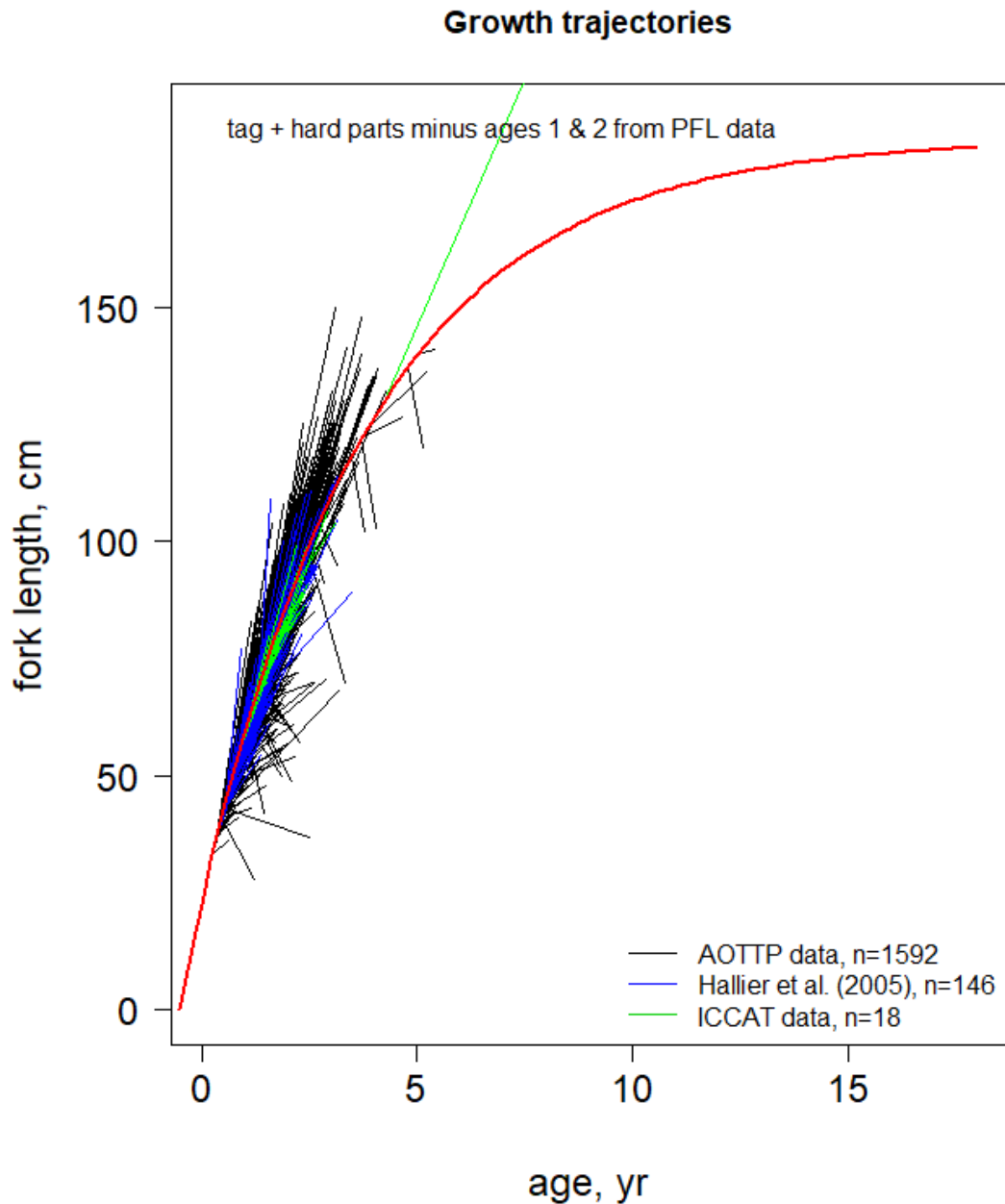


452



453 *Figure 11b. Vector plot of the tagging data from AOTTP, Hallier et al. (2005) and ICCAT. The*  
454 *vector plot is made by computing the predicted age for the length at tagging using the estimated*  
455 *von Bertalanffy growth parameters, and then assuming the age at recapture is the predicted age*  
456 *at tagging plus the time at liberty. The von Bertalanffy curve is based on the integrated model*  
457 *applied to the data without age-1 and age-2 fish from the PFL otolith dataset. The fastest*  
458 *growing 1% and the slowest growing 1% (in cm/wk) of the records have been eliminated from*  
459 *the AOTTP tagging data. One obvious outlier is seen among the 18 records from ICCAT tagging*  
460 *data; this record was not used to fit the von Bertalanffy model.*

461



462

### 463 3.3. Integrated Analysis Results

464

465 The dataset consists of 1,592 tag-recovery pairs from the AOTTP database, 18 tag-recovery pairs  
466 from ICCAT data, 146 tag-recovery pairs from Hallier dataset, 63 length-age pairs from AOTTP  
467 otoliths, 153 length-age pairs from otoliths from the Hallier dataset, 229 length-age pairs from  
468 PFL otoliths, and 12 length-age pairs from the PCL otoliths. Complete results with estimates for  
469 all of the parameters (fixed, estimated, and derived) can be found in (Table 1 of Appendix 3).

470 The results from the Richards (Schnute with  $p < 1$ ) and Von Bertalanffy (Schnute with  $p = 1$ )  
471 models were identical, and the Richards model estimated  $p = 1.000$  (Table 1 of Appendix 3).

472 A sensitivity analysis was conducted on the influence of the 41 large age-1 and age-2 fish from  
473 the PFL dataset. The integrated model was fitted to the otolith data minus the 41 PFL fish (Table  
474 4, Figure 10, and Table 2 of Appendix 3). The integrated models, with or without the deletion of  
475 PFL's age 1 and age 2 fish, had higher asymptotic sizes than the corresponding models based just  
476 on the otolith data. All six of the oldest fish were below the integrated model curves. Similar to  
477 the results from the otolith only data, the removal of the large age-1 and age-2 fish from the  
478 integrated model caused the estimate of asymptotic length to increase and the estimate of  $K$  to  
479 decrease. However, in the integrated model, the estimate of the time-axis intercept became less  
480 negative when the age-1 and age-2 PFL fish were removed (Table 4).

481 Goodness of fit of the von Bertalanffy growth model from the integrated analysis with PFL age-1  
482 and age-2 fish removed can be observed in Figure 10 (green line) and Figure 11. The integrated  
483 model describes the growth of young bigeye well but the growth of older fish tends to be above  
484 the predicted line (Figure 11b). Otoliths for the six oldest fish, four from the PCL data and two  
485 from the PFL data, are below the fitted growth curves with and without the 1 and 2year olds  
486 from PFL's data (Figure 10). The vast majority of the data (nearly 100% of tagging and ~95% of  
487 length-age pairs) come from fish age-5 or younger.

488 The von Bertalanffy curve from just the otolith data (with age-1 and age-2 fish from PFL's  
489 otolith data removed) was plotted with the tagging data (Figure 11a). This model fits the fish  
490 tagged at an older age better than the integrated model, but overestimates the growth for fish  
491 tagged at a young age with short times at liberty.

492

#### 4. Discussion

By utilizing data from both tagging studies and length-age pairs we were able to estimate several models for growth of bigeye tuna in the Atlantic Ocean. We incorporated multiple datasets to estimate a comprehensive growth model for the species.

The estimates of length measurement error in the AOTTP tagging data (roughly 7 cm) are similar to those found by Ailloud et al. (2014) for Bluefin tuna, i.e., roughly 5 cm. Measurement error in the tagging study of Hallier et al. (2005) was about 4.8 cm, slightly better than that in the AOTTP bigeye tuna data and the Bluefin tuna data. Unfortunately, the ICCAT tagging database for bigeye tuna contains very few short-term recaptures making it difficult to assess measurement error. Visual examination of the ICCAT tagging data (Figure 11) showed one obvious outlier and slightly slower growth than the tagging data of Hallier et al. (2005) and the ICCAT tagging data. There was no justification why these 17 records (after removal of the outlier) were invalid so they were retained in the analysis.

The integrated model runs yielded similar results between Richards and Von Bertalanffy when using the same datasets, i.e., the estimated value of the shape parameter  $p$  was close to or equal to the value of 1.0 at which the Schnute model reverts to a von Bertalanffy curve. The integrated model run using the von Bertalanffy model and all of the data (Table 4) estimates an  $L_{\infty}$  of 178.70 cm FL (SD 5.906) and  $K$  of 0.271 yr<sup>-1</sup> (SD 0.015). The integrated model run removing PFL's age-1 and age-2 fish estimates an  $L_{\infty}$  of 185.78 cm FL (SD 6.298) and a  $K$  of 0.252 yr<sup>-1</sup> (SD 0.014). These results are similar to those found in previous studies (Figure 1 of Appendix 1). It is worth noting that there was only one other integrated study completed for bigeye using tagging and otolith data (Hallier et al. 2005). The integrated results from that study yielded a larger estimate of  $L_{\infty}$  (217.28 cm FL) and a smaller estimated  $K$  (0.180 yr<sup>-1</sup>). One explanation is that Hallier used daily ring readings for the otoliths beyond 1 year, a practice which has been shown to be unreliable for bigeye (Williams et al. 2013, Krusic-Golub and Ailloud n.d.). The Hallier study also used a much shorter time at liberty cutoff (14 days) versus the 98 days used here, had few old fish, and few long-term recaptures. Our results are more similar to the SS3 fits to the Hallier et al. 2005 data used by the 2018 ICCAT bigeye stock assessment (Anon. 2019)  $L_{\infty} = 179.9$  and  $K = 0.281$ .

522 Of particular note is that we were able to extend the maximum age used in the analysis up to 17  
523 years compared to the maximum age of approximately 9 years used by Hallier et al. (2005) to  
524 estimate the growth parameters currently used in the stock assessment and the maximum age of 8  
525 found in the study by Delgado de Molina and Santana (1986). The importance of this is  
526 amplified by the lack of tag returns from either very large fish or fish at liberty for a very long  
527 time, i.e., from old fish.

528 Normally, it would be prudent to analyze different data sources independently to identify any  
529 conflicts among data sources. However, when fitting an asymptotic growth model, it is essential  
530 to have a wide contrast in the independent variable, age. It is impossible to judge the rate of  
531 curvature with change in age if age does not change (much) among observations. Lack of old  
532 animals in a growth study often leads to extremely high estimates of asymptotic size whereas  
533 lack of young animals can lead to very large, negative estimates of the  $t_0$  parameter. In the case  
534 of bigeye tuna, the use of multiple datasets captured a broad size spectrum of the population but  
535 the use of just the tagging data resulted in very few large, old fish.

536 The study of Hallier et al. (2005) used otoliths and tagging data while the study of Delgado de  
537 Molina and Santana (1986) used growth rings in dorsal spines. The latter authors noted problems  
538 with remodeling of the central cavity of the spine which resulted in the loss of rings representing  
539 the first years of life. Given the current study utilized several datasets over more than two  
540 decades, contained the widest range of sizes, and included validated ages beyond those currently  
541 assumed by ICCAT, this new curve should represent the most realistic estimates of bigeye tuna  
542 growth in the Atlantic to date.

543 The new curve with tagging and otolith data is similar to the curve used in the last stock  
544 assessment but with a lower estimated asymptotic size (Figure 1). The six oldest fish in the study  
545 are below the estimated growth curve which suggests that the addition of additional old fish (> 7  
546 yr, implying an effort to sample fish > 150 cm FL) to the analysis might bring the asymptotic  
547 size down and increase the growth coefficient  $K$  estimate.

548 Additional old fish should be collected (both from tagging and length-age data) in order to better  
549 estimate the model. The curve based on otolith data (without PFL's age 1 and age 2 fish) goes  
550 through the cloud of six old fish on the right. In the absence of adequate samples of old (large)  
551 fish, one can artificially assign greater weight to the existing samples of old fish to force the

552 curve to go through the cloud of data points of old fish (e.g., Maunder et al. 2018). We estimated  
553 the growth parameters  $K$  and  $t_0$  with  $L_\infty$  held fixed at various values (Appendix 5). This shows  
554 that the asymptotic size is not well determined, with fits having  $L_\infty$  fixed anywhere between 155  
555 and 170 cm FL having similar residual standard errors when age 1 and age 2 PFL fish are  
556 removed from the dataset.

557 All of the tagging data appear to be in some conflict with the otolith data (Figure 11a, 11b).  
558 When the vector plot is made with the curve fitted to just otolith data (Figure 11a), the young  
559 fish appear to grow slower than predicted by the growth curve as evidenced by the observation  
560 that there are more termini of the vectors to the right (below) the fitted line than to the left  
561 (above); fish recaptured at an older age (age > 2) tend to be to the left (above) the fitted line. This  
562 suggests a conflict between the tagging and otolith results. When the curve is fitted to tagging  
563 and otolith data, a different pattern appears in the vector plot (Figure 11b). Now, the vectors for  
564 fish tagged at age 0 and age 1 appear to be symmetric about the regression line, but the lack of fit  
565 for fish recaptured at age > 2 is worse than in Figure 11a.

566 It is not clear why the tagging and otolith data are in disagreement. We propose the model based  
567 on otolith data provides the most realistic estimates of bigeye tuna growth because it predicts the  
568 size of old fish through the fitted value of  $L_\infty$  and it avoids patterns in the residuals from the  
569 tagging data (Appendix 4). If tagged bigeye tuna with longer times at liberty are recaptured in  
570 the future it could resolve the apparent discrepancy between the tagging and otolith data. The  
571 inclusion of additional otoliths and tag returns from old fish would improve both models as the  
572 sample size for old fish remains limited.

573

#### 574 **Acknowledgements**

575 We thank members of the AOTTP tag and recovery teams, including biological samplers, for  
576 doing the meticulous work of otolith extraction in recovered fish. We thank Captains Billy  
577 McIntyre of the F/V Shady Lady, Dan Mears Jr. of the F/V Monica, and their respective crew  
578 who were vital for longline sampling efforts and personal communications regarding fishery  
579 dynamics. Officials and participants in the Oak Bluffs Bluewater Classic, Mid-Atlantic Tuna,  
580 Ocean City Tuna, White Marlin Open, and Mid-Atlantic Billfish tournaments were also crucial  
581 for obtaining samples. Graduate students and lab technicians, Kelsey Moon, Isabelle See,  
582 Samantha Nadeau, and Brenda Rudnicky assisted with field and lab work for this project as well.  
583 Funding to support biological sampling of tunas, age estimation and radiocarbon analysis was

584 provided by NOAA CRP # NA17NMF4540140 to Walt Golet in the School of Marine Sciences  
585 at the University of Maine. This work was also supported by the European Union (DCI-  
586 FOOD/2015/361-161). Additional financial support from ICCAT Contracting Parties and  
587 Cooperating non-Contracting Parties is gratefully acknowledged. Funding provided for L.  
588 Waterhouse and J. Hoenig by International Commission for the Conservation of Atlantic Tunas  
589 under fiscal identification number N4001546C. The anonymous reviewers and Beth Matta  
590 provided helpful comments.

591 **References**

- 592 Ailloud, L. E., M. V. Laretta, J. M. Hoenig, J. F. Walter, and A. Fonteneau. 2014. Growth of Atlantic  
593 Bluefin Tuna Determined From the ICCAT Tagging Database: A Reconsideration of Methods.  
594 *Collective Volume of Scientific Papers. ICCAT. 70:380–393.*
- 595 Ailloud, L.E., M.V. Laretta, A.R.Hanke, W.J. Golet, R. Allman, M.R. Siskey, D.H. Secor, and J.M.  
596 Hoenig. 2017. Improving growth estimates for western Atlantic Bluefin tuna using an integrated  
597 modeling approach. *Fisheries Research. 191:17-24.*
- 598 Ailloud, L.E., Beare, D., Farley, J.H. and Krusic-Golub, K., 2019. Preliminary results on AOTTP  
599 validation of otolith increment deposition rates in yellowfin tuna in the Atlantic. *Collective Volume*  
600 *of Scientific Papers. ICCAT. 76(6):156-163.*
- 601 Aires-da-Silva, A.M., M.N. Maunder, K.M. Schaefer, D.W. Fuller. 2015. Improved growth estimates  
602 from integrated analysis of direct aging and tag-recapture data: an illustration with bigeye tuna  
603 (*Thunnus obesus*) of the eastern Pacific Ocean with implications for management. *Fisheries*  
604 *Research. 163:119-126.*
- 605 Allman, R., Ailloud, L., Austin, R., Falterman, B., Farley, J., Lang, E., Pacicco, A., & Satoh, K. (2020).  
606 Report of the International Workshop On the Ageing of Yellowfin and Bigeye Tuna. *Collective*  
607 *Volume of Scientific Papers. ICCAT. 77(8), 32–46.*
- 608 Alves, A., P. de Barros, and M. R. Pinho. 2002. Age and growth studies of bigeye tuna *Thunnus obesus*  
609 from Madeira using vertebrae. *Fisheries Research. 54:389–393.*
- 610 Andrews, A. H., A. Pacicco, R. Allman, B. J. Falterman, E. T. Lang, and W. Golet. 2020. Age validation  
611 of yellowfin (*Thunnus albacares*) and bigeye (*Thunnus obesus*) tuna of the northwestern atlantic  
612 ocean. *Canadian Journal of Fisheries and Aquatic Sciences. 77:637–643.*
- 613 Anon. 2019. Report of the 2018 ICCAT Bigeye Tuna Stock Assessment Meeting. *Collective Volume of*  
614 *Scientific Papers. ICCAT. 75(7): 1721-1855.*
- 615 Anon. 2021. ICCAT Atlantic Ocean tropical Tuna Tagging Programme (AOTTP) evidence based  
616 approach for sustainable management of tuna resources in the Atlantic. Final Report. Available  
617 at: [https://www.iccat.int/aottp/AOTTP-Documents/Reports/Interim-Report/AOTTP-Interim-](https://www.iccat.int/aottp/AOTTP-Documents/Reports/Interim-Report/AOTTP-Interim-Report-2019.pdf)  
618 [Report-2019.pdf](https://www.iccat.int/aottp/AOTTP-Documents/Reports/Interim-Report/AOTTP-Interim-Report-2019.pdf).
- 619 Baty, F., C. Ritz, S. Charles, M. Brutsche, J.-P. Flandrois, and M.-L. Delignette-Muller. 2015. A Toolbox  
620 for Nonlinear Regression in R: The Package nlstools. *Journal of Statistical Software. 66:1–21.*
- 621 Beare, D., L. E. Ailloud, J. Garcia, R. Pastor, and S. Kebe. 2019. ICCAT Atlantic Ocean tropical Tuna  
622 Tagging Programme (AOTTP) : Evidence based approach for sustainable management of tuna  
623 resources in the Atlantic. Available at: [https://www.iccat.int/aottp/AOTTP-Documents-](https://www.iccat.int/aottp/AOTTP-Documents/Reports/Interim-Report/AOTTP-Interim-Report-2019.pdf)  
624 [Library/Reports/Interim-Report/AOTTP-Interim-Report-2019.pdf](https://www.iccat.int/aottp/AOTTP-Documents/Reports/Interim-Report/AOTTP-Interim-Report-2019.pdf)
- 625 Busawon, D.S., E. Rodriguez-Marin, P.L. Luque, R. Allman, B. Gahagan, W. Golet, E. Koob, M. Siskey,  
626 M.R. Sobrón, P. Quelle, J. Nielson, and D.H. Secor. 2015. Evaluation of an Atlantic bluefin tuna  
627 otolith reference collection. *Collective Volume of Scientific Papers. ICCAT. 71(2): 960-982.*
- 628 Cayré, P., J. B. Amon Kothias, T. Diouf, and J. M. Stretta. 1993. Biology of tuna. Pages 147–244 in A.  
629 Fonteneau and J. Marcille, editors. Resources, fishing and biology of the tropical tunas of the  
630 Eastern Central Atlantic. FAO Fisher. FAO, Rome.
- 631 Cayré, P., and T. Diouf. 1984. Croissance du thon obèse (*Thunnus obesus*) de l’atlantique d’après les  
632 resultats de marquage. *Collective Volume of Scientific Papers. ICCAT. 20:180–187.*

- 633 Champagnat, C., and R. Pianet. 1974. Croissance du Fatudo (*Thunnus obesus*) Dans Les Recions de  
634 Dakar et de Pointe-Noire *Collective Volume of Scientific Papers. ICCAT.* 2:141–144.
- 635 Collette, B. B., and C. E. Nauen. 1983. FAO species catalogue. Scombrids of the world. An annotated and  
636 illustrated catalogue of tunas mackerels, bonitos and related species know to date.
- 637 Delgado de Molina, A., and J. C. Santana. 1986. Estimacion de la edad y crecimiento del patudo  
638 (*Thunnus obesus*, Lowe 1939) capturado en las islas canarias. *Collective Volume of Scientific*  
639 *Papers. ICCAT.* 25:130–137.
- 640 Draganik, B., and W. Peiczarski. 1984. Growth and Age of Bigeye and Yellowfin Tuna in the Central  
641 Atlantic as Per Data Gathered by R/V Wicczno. *Collective Volume of Scientific Papers. ICCAT.*  
642 20:96–103.
- 643 Eveson, J.P., Laslett, G.M., Polacheck, T., 2004. An integrated model for growth incor-porating tag-  
644 recapture, length-frequency, and direct aging data. *Canadian Journal of Fisheries and Aquatic*  
645 *Sciences.* 61:292-306.
- 646 Farley, J. H., Clear, N. P., Leroy, B., Davis, T. L. O., & McPherson, G. (2006). Age, growth and  
647 preliminary estimates of maturity of bigeye tuna, *Thunnus obesus*, in the Australian region. *Marine*  
648 *and Freshwater Research.* 57(7):713–724. <https://doi.org/10.1071/MF05255>
- 649 Farley, J.H., N.P. Clear, D. Kolody, K. Krusic-Golub, P. Eveson, and J. Young. (2016). Determination of  
650 swordfish growth and maturity relevant to the southwest Pacific stock. WCPFC-SC12-2016/SAWP-  
651 11.
- 652 Farley, J., K. Krusic-Golub, N. Clear, P. Eveson, N. Smith, and P. Hampton. 2019. Project 94: Workshop  
653 on yellowfin and bigeye age and growth. WCPFC-SC15-2019/SA-WP-02. Available at:  
654 [https://spccfpstore1.blob.core.windows.net/digitallibrary-  
655 docs/files/a2/a2924c5afcea64f140f40f6e66918601.pdf?sv=2015-12-  
656 11&sr=b&sig=CwYqjW53CyG7R0E488sXfJS5d%2BPTC%2B72wZUkVbkF0bl%3D&se=2022-  
657 06-11T21%3A31%3A08Z&sp=r&rscc=public%2C%20max-age%3D864000%2C%20max-  
658 stale%3D86400&rsct=application%2Fpdf&rscd=inline%3B%20filename%3D%22SC15\\_SA\\_WP\\_0  
659 2\\_Project\\_94\\_WS\\_on\\_YFT\\_and\\_BET\\_age\\_and\\_growth.pdf%22](https://spccfpstore1.blob.core.windows.net/digitallibrary-docs/files/a2/a2924c5afcea64f140f40f6e66918601.pdf?sv=2015-12-11&sr=b&sig=CwYqjW53CyG7R0E488sXfJS5d%2BPTC%2B72wZUkVbkF0bl%3D&se=2022-06-11T21%3A31%3A08Z&sp=r&rscc=public%2C%20max-age%3D864000%2C%20max-stale%3D86400&rsct=application%2Fpdf&rscd=inline%3B%20filename%3D%22SC15_SA_WP_02_Project_94_WS_on_YFT_and_BET_age_and_growth.pdf%22)
- 660 Fournier, D.A., H. J. Skaug, J. Ancheta, J. Ianelli, A. Magnusson, M. N. Maunder, A. Nielsen, and J.  
661 Sibert. 2012. AD Model Builder: using automatic differentiation for statistical inference of highly  
662 parameterized complex nonlinear models. *Optimization Methods and Software.* 27:233–249.
- 663 Francis, R.I.C.C., 1988a. Maximum likelihood estimation of growth and growth variability from tagging  
664 data. *New Zealand journal of marine and freshwater research,* 22(1), pp.43-51.
- 665 Francis, R.I.C.C., 1988b. Are growth parameters estimated from tagging and age-length data  
666 comparable?. *Canadian Journal of Fisheries and Aquatic Sciences.* 45(6):936-942.
- 667 Francis, R.I.C.C., A.M. Aires-da-Silva, M.N. Maunder, K.M. Schaefer, and D.W. Fuller. 2016.  
668 Estimating fish growth for stock assessments using both age-length and tagging-increment data.  
669 *Fisheries Research.* 180: 113-118.
- 670 Gaikov, V. V., V. N. Chur, V. L. Zharov, and Y. P. Fedoseev. 1980. On Age and Growth of Atlantic  
671 Bigeye Tuna. *Collective Volume of Scientific Papers. ICCAT.* 9:294–302.
- 672 Hallier, J.-P., B. Stequert, O. Maury, and F.-X. Bard. 2005. Growth of bigeye tuna (*Thunnus obesus*) in  
673 the eastern atlantic ocean from tagging-recapture data and otolith readings. *Collective Volume of*  
674 *Scientific Papers. ICCAT.* 57:181–194.



675 ICCAT Secretariat. (n.d.). Access to ICCAT statistical databases.  
676 <https://www.iccat.int/en/accesingdb.html>.

677 IOTC Secretariat. 2006. Biological data on tuna and tuna-like species gathered. IOTC-2006-WPB-INF01.  
678 at the IOTC Secretariat: Status Report | IOTC.

679 Krusic-Golub, K., and L. E. Ailloud. (n.d.). Evaluating otolith increment deposition rates in Atlantic  
680 Ocean bigeye and yellowfin tuna tagged during the Atlantic Ocean tropical Tuna Tagging Program.

681 Lang, E.T., B.J. Falterman, L.L Kitchens, and C.D. Marshall. (2017). Age and growth of Yellowfin Tuna  
682 (*Thunnus albacares*) in the northern Gulf of Mexico. *Collective Volume of Scientific Papers*.  
683 *ICCAT*. 73(1): 423-433.

684 Laslett, G.M., Eveson, J.P. and Polacheck, T., 2002. A flexible maximum likelihood approach for fitting  
685 growth curves to tag recapture data. *Canadian Journal of Fisheries and Aquatic Sciences*,  
686 59(6):976-986.

687 Marcille, J., C. Champagnat, and N. Armada. 1978. Croissance du patudo (*Thunnus obesus*) de l'Océan  
688 Atlantique intertropical oriental. *Documents Scientifiques, Centre de Recherches*  
689 *Océanographiques, Abidjan*. 9:73–81.

690 Maunder, M. N., Deriso, R. B., Schaefer, K. M., Fuller, D. W., Aires-da-Silva, A. M., Minte-Vera, C. V.,  
691 and S. E. Campana. 2018. The growth cessation model: a growth model for species showing a near  
692 cessation in growth with application to bigeye tuna (*Thunnus obesus*). *Marine Biology*. 165(76).  
693 <https://doi.org/10.1007/s00227-018-3336-9>

694 Ogle DH, Doll JC, Wheeler P, Dinno A (2021). *FSA: Fisheries Stock Analysis*. R package version 0.9.1,  
695 <https://github.com/droglenc/FSA>.

696 R Core Team. 2020. R: A Language and Environment for Statistical Computing. R Foundation for  
697 Statistical Computing, Vienna, Austria.

698 Richards, F. J. 1959. A flexible growth function for empirical use. *Journal of Experimental Botany*  
699 10:290–301.

700 Rodríguez-Marín, E., Landa, J., Ruiz, M., Godoy, D., and Rodríguez- Cabello, C. (2004). Age estimation  
701 of adult bluefin tuna (*Thunnus thynnus*) from dorsal spine reading. *Collective Volume of Scientific*  
702 *Papers. ICCAT*. 56:1168–1174.

703 Schnute, J., 1981. A versatile growth model with statistically stable parameters. *Canadian Journal of*  
704 *fisheries and aquatic sciences*. 38(9):1128-1140.

705 Schnute, J. T., and L. J. Richards. 1990. A unified approach to the analysis of fish growth, maturity, and  
706 survivorship data. *Canadian Journal of Fisheries and Aquatic Sciences*. 47:24–40.

707 Scida, P., A. Rainosek, and T. Lowery. 2001. Length conversions for yellowfin tuna (*Thunnus albacares*)  
708 caught in the western north atlantic ocean. *Collective Volume of Scientific Papers. ICCAT*. 52:528–  
709 532.

710 Von Bertalanffy, L. 1938. A quantitative theory of organic growth (inquiries on growth laws. II). *Human*  
711 *Biology*. 10:181–213.

712 Weber, E. 1980. An Analysis of Atlantic Bigeye Tuna (*Thunnus obesus*) Growth. *Collective Volume of*  
713 *Scientific Papers. ICCAT*. 9:303–307.

714 Williams, A. J., B. M. Leroy, S. J. Nicol, J. H. Farley, N. P. Clear, K. Krusic-Golub, C. R. Davies. 2013.  
715 Comparison of daily- and annual- increment counts in otoliths of bigeye (*Thunnus obesus*),

716 yellowfin (*T. albacares*), southern bluefin (*T. maccoyii*) and albacore (*T. alalunga*) tuna. *ICES*  
717 *Journal of Marine Science*. 70:1439-1450.

## Appendices

### Appendix 1

Appendix 1, Table 1. Estimates of growth parameters for bigeye tuna in the Atlantic Ocean.  $L_{\infty}$  and Length Range pertain to fork length in cm;  $K$  is in units of  $yr^{-1}$  and  $t_{\infty}$  is in yr.

Growth Function	Linf	K	$t_{\infty}$	Length Range	Method	Reference
VB	161.21	0.392	-0.239	29 – 175	Otoliths	This study
VB	185.78	0.252	-0.524	28 - 175	Otoliths, tagging	This study
Peterson's method	338.53	0.10497	-0.5425	58 - 140	Length Frequency (predorsal)	Champagnat & Pianet 1974
VB	199.77	0.1970	-0.71		Spines, males (n=245)	Delgado de Molina & Santana 1986
VB	214.54	0.1669	-0.77		Spines, females (n=239)	Delgado de Molina & Santana 1986
VB	206.14	0.1822	-0.74	50 - 180	Spines, both sexes (n=540)	Delgado de Molina & Santana 1986
VB	253.75	0.173	-0.15		Spines	Gaikov et al. 1980
VB	491.6	0.0135	3.808	40 - 180	Length Frequency	Weber 1980
VB	218.8	0.23	-0.20	56 - 190	Spines (n=77)	Draganik & Peiczarski 1984
VB	195.54	0.206		37 – 124	Tagging (n=625)	Hallier et al. 2005
VB (solved in excel)	207.43	0.202	-0.613	29 -190	Otoliths, daily (n=230)	Hallier et al. 2005
VB (FAO vonbit)	206.976	0.203	-0.616	29 -190	Otoliths, daily (n=230)	Hallier et al. 2005
Gompertz	179.13	0.4088	(A= 1.7268)	29 -190	Otoliths, daily (n=230)	Hallier et al. 2005
Richards	178.63	0.424	(b= -7.185, m= 2280.4)	29 -190	Otoliths, daily (n=230)	Hallier et al. 2005
VB	217.28	0.180	-0.709	37 – 124 & 29 -190	Tagging (n=625) & Otoliths, daily (n=230). Used in last stock assessment.	Hallier et al. 2005
VB	264.02	0.12	-0.68	44 – 179	Caudal vertebrae (n=175)	Alves et al. 2002
VB	285.3745	0.1127			Tagging (n=243)	Cayre and Diouf 1984
VB / Petersen's method	249.6	0.0124	-4.78		Length frequency	Marcille et al. 1978

## Appendix 2

Appendix 2, Table 1. Modified from Table 1 in IOTC Secretariat 2006 and Scida et al. 2001. Definition of length measurements used in conversions for tuna lengths (Table 2 of Appendix 2).

Length	Type	Description
CFL	Curved fork length	
CKL	Cleithrum-Keel length	Projected straight distance between the point on the cleithrum that provides the shortest possible measurement to the anterior portion of the caudal keel. The cleithrum is the semicircular bony structure at the posterior edge of the gill opening.
EYF	Eye to fork	
FL	Fork Length	Projected straight distance from the tip of the upper jaw (snout) to the shortest caudal ray (fork)
FLT	Curved Fork Length	Projected curved-body distance from the tip of the upper jaw (snout) to the shortest caudal ray (fork).
LD1	Lower jaw to 1 <sup>st</sup> dorsal	
LJF	Lower Jaw Fork Length	**Equivalent to fork length for tropical tuna species.
PFL	Pectoral-fork length	Projected straight distance between the most anterior insertion of the pectoral fin and the fork of the tail.
PFLT	Curved Pectoral-fork length	Projected curved-body distance between the most anterior insertion of the pectoral fin and the fork of the tail.
SFL	Straight fork length	**Equivalent to fork length for tropical tuna species.
SL	Snout (preorbital) length	
STD	Standard length	
TLE	Total length	
UNK	Unknown	

Appendix 2, Table 2. Length conversions used to convert between different length standards. Acronyms and definitions are given in Table 1 of Appendix 2.

L	a	b	R2	Standard Length ( $Y = a+b*L$ )	Area	Range (cm)	n	Ref
PFL	18.191	1.2129	0.8988	FL	Atl.	33-141	3174	1
CKL	-5.5109	0.6215	0.9255	FL	Atl.	29-110	570	1
PFLT	-2.287	1.4572	0.9564	FL	Atl.	44-110	59	1
PFLT	7.1818	1.3418	0.9733	FLT	Atl.	44-110	59	1
FLT	0.9082	0.9676	0.9891	FL	Atl.	63-169	304	1

### Appendix 3.

Complete results from fitting the integrated model to all of the data (Table 1 Appendix 3) and to the data with age-1 and age-2 fish from PFL data removed (Table 2 Appendix 3).

*Appendix 3, Table 1. Results from Richards and Von Bertalanffy models fitted to the full data set consisting of tagging data from AOTTP, ICCAT, and the Hallier et al. (2005) study plus hard part data from AOTTP, Hallier (only ages < 1 yr), PFL data, and PCL data. Symbols are defined in the main text. Note that  $p$  is fixed at 1.0 in the von Bertalanffy model and estimated to be 1.000 in the Richards model.*

	Richards		Von Bertalanffy	
	(Schnute with $ p  < 100$ )		(Schnute with $p = 1$ )	
	Value	S.E.	Value	S.E.
<b>Fixed parameters</b>				
$A_1$	0	-	0	-
$A_2$	17	-	17	-
$p$	-	-	1	-
<b>Estimated parameters</b>				
$L_1$	24.364	0.765	24.364	0.765
$L_2$	178.910	5.560	178.910	5.560
$K$	0.266	0.015	0.266	0.015
$p$	1.00	8.867e-08	-	-
$k_\rho$	1.381	0.232	1.381	0.232
$\rho_0$	0.887	0.015	0.887	0.015
$\sigma_{L_1}$	2.220	0.387	2.220	0.387
$\sigma_{L_2}$	26.713	1.063	26.713	1.063
$\mu_{\log A_{tag}}$	-0.187	0.020	-0.187	0.020
$\sigma_{\log A_{tag}}$	-1.068	0.034	-1.068	0.034
<b>Derived parameters</b>				
$L_\infty$	180.590	6.046	180.590	6.046
$t_0$	-	-	-0.544	0.028
$t^*$	-0.544	0.028	-	-
$a^*$	-1.641	0.500	-1.641	0.500
$b^*$	0.158	7.711e-03	0.158	7.711e-03
$b$	-1.000	7.679e-08	-	-
<b>Negative log-likelihood</b>	9238.97945		9238.97945	

*Appendix 3, Table 2. Results from Richards and Von Bertalanffy models fitted to the full data set consisting of tagging data from AOTTP, ICCAT, and the Hallier et al. (2005) study plus hard part data from AOTTP, Hallier (only ages < 1 yr), PFL data, and PCL data. Symbols are defined in the main text. The age-1 and age-2 fish have been removed from PFL ( $n=41$ ) to avoid*

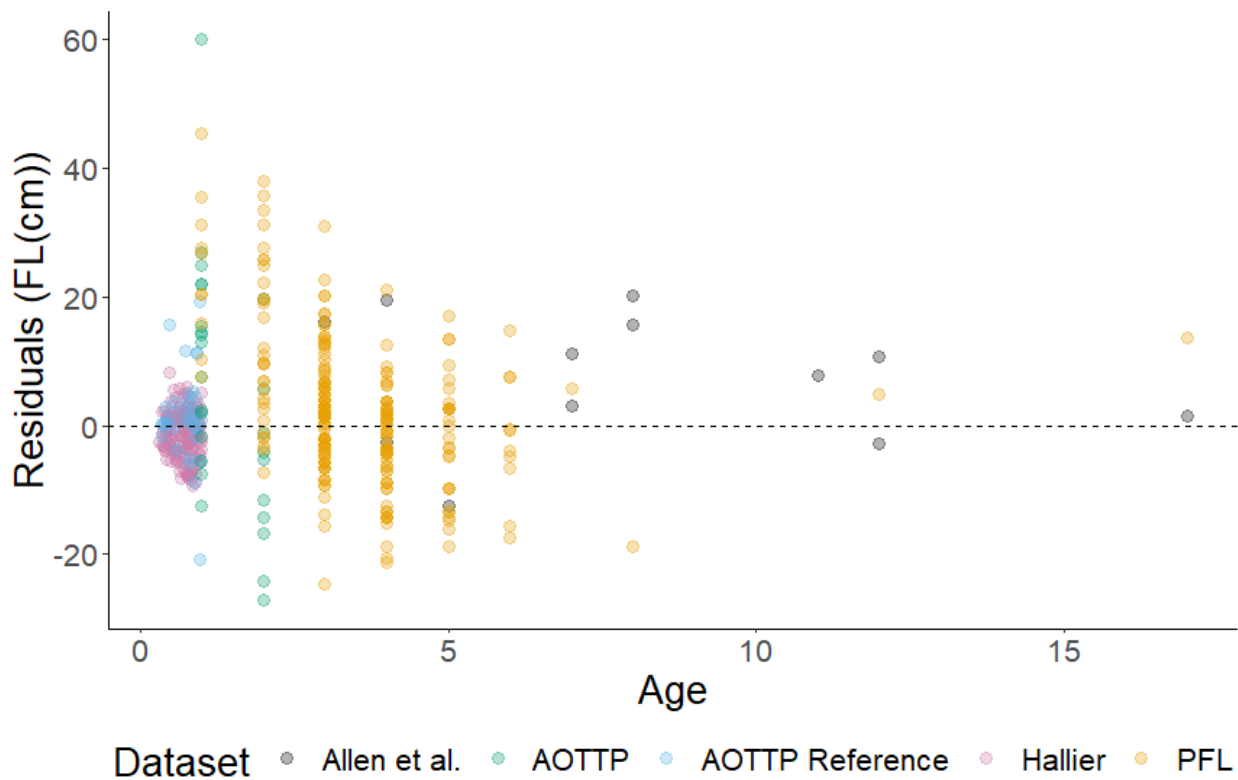
probable sampling bias. Note that  $p$  is fixed at 1.0 in the von Bertalanffy model and estimated to be 1.000 in the Richards model.

	Richards		Von Bertalanffy	
	(Schnute with $ p  < 100$ )		(Schnute with $p = 1$ )	
	Value	S.E.	Value	S.E.
<b>Fixed parameters</b>				
$A_1$	0	-	0	-
$A_2$	17	-	17	-
$p$	-	-	1	-
<b>Estimated parameters</b>				
$L_1$	23.127	0.642	23.127	0.642
$L_2$	185.450	5.790	185.450	5.790
$K$	0.247	0.014	0.247	0.014
$p$	1.000	1.317e-07	-	-
$k_\rho$	1.434	0.253	1.434	0.253
$\rho_0$	0.864	0.019	0.864	0.019
$\sigma_{L_1}$	1.571	0.322	1.571	0.322
$\sigma_{L_2}$	26.297	1.074	26.297	1.074
$\mu_{\log A_{tag}}$	-0.132	0.017	-0.132	0.017
$\sigma_{\log A_{tag}}$	-1.076	0.031	-1.076	0.031
<b>Derived parameters</b>				
$L_\infty$	187.900	6.455	187.900	6.455
$t_0$	-	-	-0.531	0.025
$t^*$	-0.531	0.025	-	-
$a^*$	-1.952	0.429	-1.952	0.429
$b^*$	0.152	7.055e-03	0.152	7.055e-03
$b$	-1.000	1.178e-07	-	-
<b>Negative log-likelihood</b>	9014.8878		9014.8878	

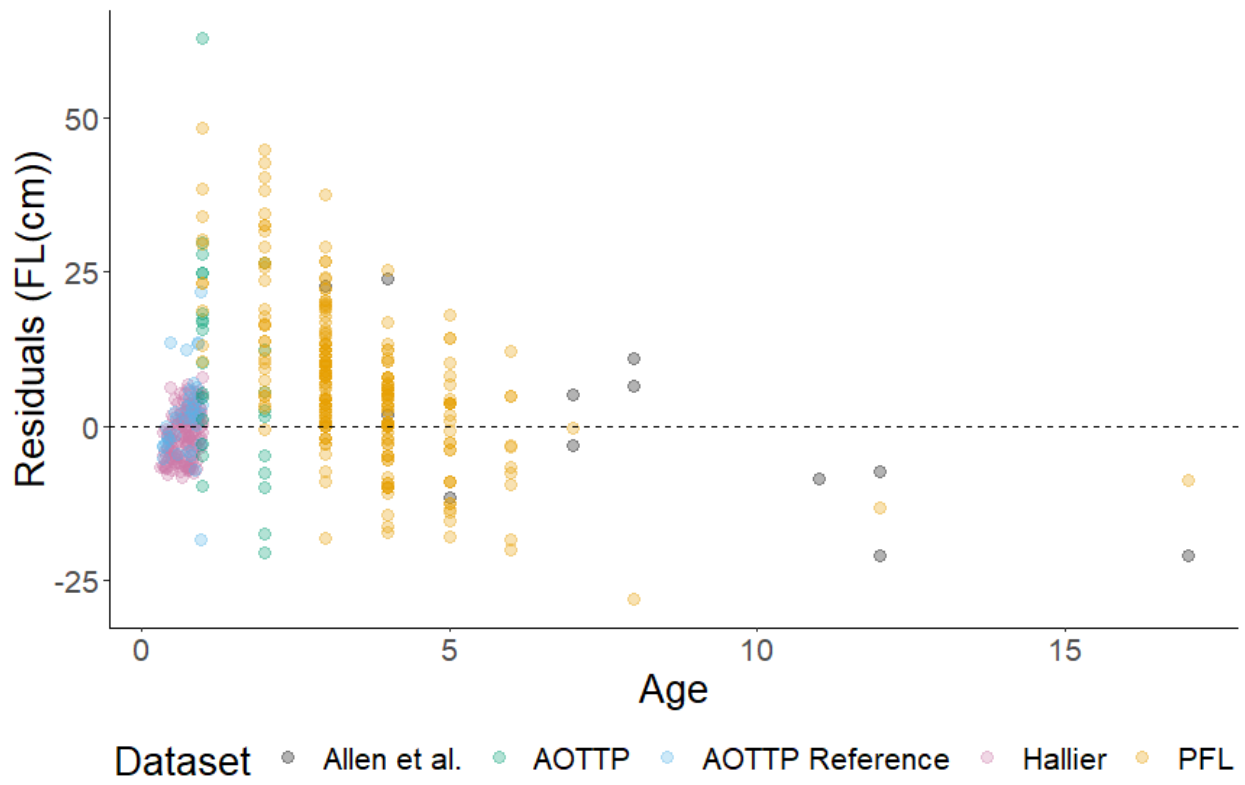
#### Appendix 4.

Residual plots from the preferred model (length-age pair data only) and the best fitting integrated model. For the preferred model (length-age pair data only), the asymptotic length  $L_{\infty}$  (fork length) equals 161.21 cm (95% bootstrap CI 154.39, 166.84), growth parameter  $K$  equals 0.392  $\text{yr}^{-1}$  (95% bootstrap CI 0.355, 0.441), and the time-axis intercept  $t_0$  equals -0.239 yr (95% bootstrap CI -0.306, -0.175). For the best fitting integrated model, the asymptotic length  $L_{\infty}$  (fork length, in cm) was estimated to be 185.78 (SD 6.298), the growth parameter  $K$  was 0.252  $\text{yr}^{-1}$  (SD 0.014), and the time-axis intercept  $t_0$  was -0.524 yr (SE 0.025).

*Appendix 4, Figure 1. Residual plot by age from the preferred model (length-age pair data only).*

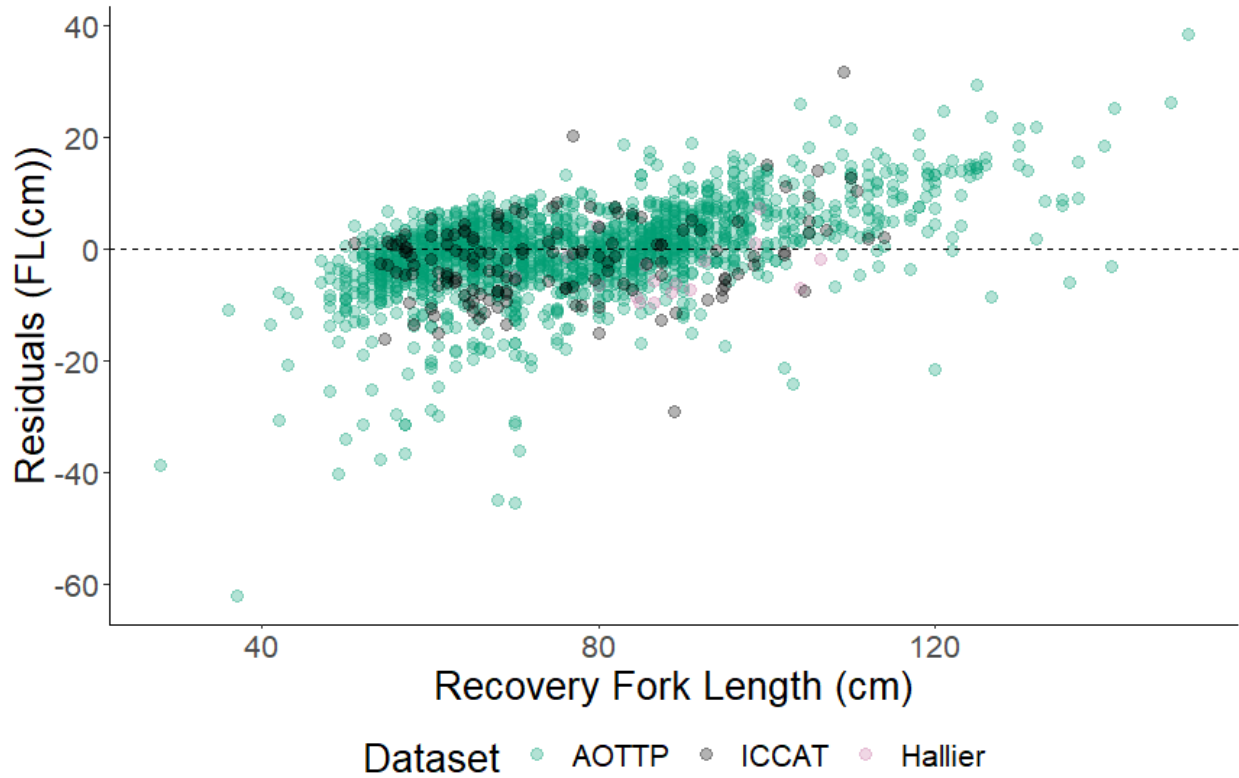


Appendix 4, Figure 2. Residual plot by age from the integrated model for the length-age pair data only.

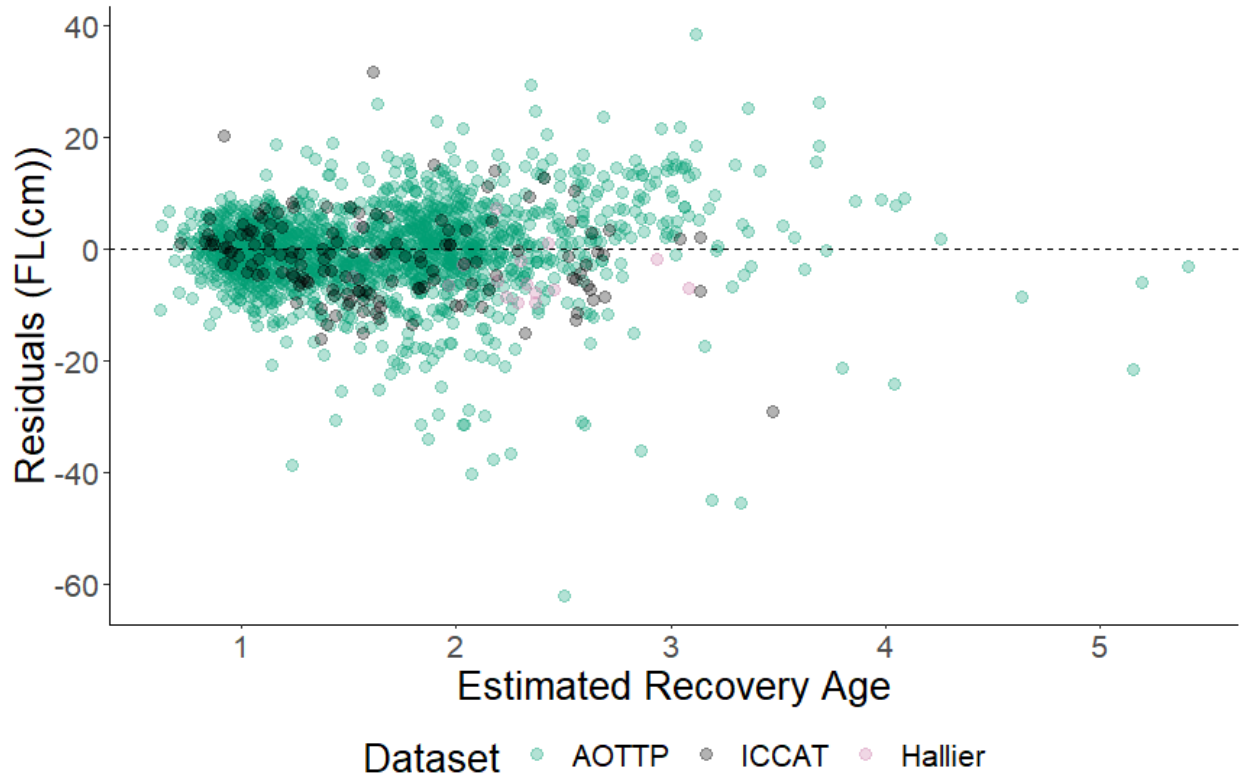




**Appendix 4, Figure 3.** Residual plot by recovery fork length (cm) from the integrated model for the tagging data only. A release age was calculated using the parameter estimates and the release fork length (cm). The recovery age was calculated by adding time at liberty to the calculated release age.



**Appendix 4, Figure 4.** Residual plot by estimated recovery age from the integrated model for the tagging data only. A release age was calculated using the parameter estimates and the release fork length (cm). The recovery age was calculated by adding time at liberty to the calculated release age.



## Appendix 5.

Parameter estimates for the von Bertalanffy growth model (length-age pair data only) were computed when the value of the asymptotic length  $L_{\infty}$  (fork length) was fixed. When the model is fit without setting a value for asymptotic length  $L_{\infty}$  and with PFL age 1 and 2 otoliths removed (Table 4), the asymptotic length  $L_{\infty}$  (fork length) equals 161.21 cm (95% bootstrap CI 154.39, 166.84), growth parameter  $K$  equals  $0.392 \text{ yr}^{-1}$  (95% bootstrap CI 0.355, 0.441), and the time-axis intercept  $t_0$  equals  $-0.239 \text{ yr}$  (95% bootstrap CI  $-0.306, -0.175$ ). From Figure 10 the values of the asymptotic length  $L_{\infty}$  (fork length) that would best fit the oldest fish would be between 165 and 175, and this would result in a value of growth parameter  $K$  between 0.368 and 0.316 (when PFL age 1 and 2 otoliths are removed) or 0.380 to 0.325 (when all otoliths are included).

*Appendix 5, Table 1. Parameter estimates from fitting von Bertalanffy models to the otolith data when fixing the value of asymptotic length  $L_{\infty}$  (fork length). This was done with otolith data when the age-1 and age-2 fish were removed from the PFL otolith data and with all otolith data. Estimated values for growth parameter  $K$  and time-axis intercept  $t_0$  and the residual standard error have been rounded to three decimal places.*

Set Value $L_{\infty}$	PFL age 1 and 2 otoliths removed			All otoliths		
	Estimated Value		Residual Standard Error	Estimated Value		Residual Standard Error
	$K$	$t_0$		$K$	$t_0$	
145	0.540	-0.078	9.292	0.564	-0.064	10.344
150	0.484	-0.130	8.987	0.505	-0.118	10.202
155	0.439	-0.180	8.817	0.456	-0.172	10.170
160	0.400	-0.228	8.752	0.415	-0.224	10.218
165	0.368	-0.274	8.769	0.380	-0.275	10.324
170	0.340	-0.319	8.850	0.351	-0.324	10.472
175	0.316	-0.362	8.980	0.325	-0.371	10.650
180	0.294	-0.403	9.147	0.302	-0.417	10.849
185	0.276	-0.443	9.341	0.283	-0.461	11.063
190	0.259	-0.481	9.555	0.265	-0.504	11.286
195	0.244	-0.519	9.782	0.249	-0.546	11.514
200	0.231	-0.555	10.018	0.235	-0.586	11.744

**Appendix 5, Figure 1.** Estimated value of von Bertalanffy growth parameter  $K$ , and residual standard error, when the curve is fit to the data without the PFL age 1 and age 2 fish and with the value of  $L_\infty$  fixed.

